A Theoretical Study on the Complete Catalytic Cycle of the Hetero-Pauson–Khand-Type [2+2+1] Cycloaddition Reaction of Ketimines, Carbon Monoxide and Ethylene Catalyzed by Iron Carbonyl Complexes

Wolfgang Imhof,*[a] Ernst Anders,*[b] Angela Göbel,[a] and Helmar Görls[a]

Dedicated to Professor Gottfried Huttner on the occasion of his 65th birthday

Abstract: The [2+2+1] cycloaddition reaction of 1,4-diazabutadienes, carbon monoxide and ethylene catalyzed by iron carbonyl complexes produces pyrrolidin-2-one derivatives. Only one of the two imine moieties is activated during the catalysis. The mechanism of this cycloaddition reaction is studied by density functional theory at the B3LYP/6-311++G(d,p) level of theory. In accordance with experimental results, a [(diazabutadiene)$Fe(CO)_3$] complex of square-pyramidal geometry is used as the starting compound **S** of the catalytic cycle. Based on experimental experience, the reaction with ethylene is considered to take place before any interaction with carbon monoxide. According to the computational results, the reaction does not proceed by ligand dissociation followed by addition of ethylene and subsequent intramolecular activation steps but by the approach of an ethylene molecule from the base of the square-pyramidal complex. This reaction yields an intermediate $\mathbf{I_4}$ in which ethylene is coordinated to the iron centre and a new C–C bond between ethylene and one of the imine groups is formed. The insertion of a terminal carbon monoxide ligand into the metal–carbon bond between ethylene and iron produces the key intermediate $\mathbf{I_7}$. The reaction proceeds by metal-assisted formation of a lactam **P**. The catalytic cycle is closed by a ligand-exchange reaction in which the diazabutadiene ligand substitutes **P** with reformation of **S**. This reaction pathway is found to be energetically favored over a reductive elimination. It leads to the experimentally observed heterocyclic product **P** and a reactive [$Fe(CO)_3$] fragment.

Keywords: cycloaddition · density functional calculations · homogeneous catalysis · iron · lactams

Introduction

Transition-metal-catalyzed cycloaddition reactions are among the most versatile methods for the synthesis of carbocyclic or heterocyclic compounds and have thus been thoroughly reviewed in past years.[1] Compared to classical methods to construct cyclic compounds, catalytic cycloaddition reactions have proven to be advantageous, especially in terms of selectivity and atom economy.

The Pauson–Khand reaction is a formal [2+2+1] cycloaddition reaction that is used for the formation of five-membered ring systems. Originally, the Pauson–Khand reaction allowed the preparation of cyclopentenones from an intramolecular reaction of an alkyne, which is introduced as an [(alkyne)$Co_2(CO)_6$] complex, with an olefin and one of the CO ligands at cobalt.[2] In the meantime, some catalytic variations of this reaction have also been developed.[3] In addition, the reaction principle may also be exceeded towards the formation of heterocyclic compounds. Thus, lactones may be generated if carbonyl compounds are used instead of the alkyne. Unsaturated lactones or lactams, respectively, are produced from CO, an alkyne and an aldehyde or an aldimine.[4] However, it must be pointed out that nearly all those reactions start from a substrate that already contains two of the functionalities used by the [2+2+1] cycloaddition reaction, which then is catalytically reacted with CO. One exception is the synthesis of functionalized γ-butyrolactones from a ketone, ethylene and CO.[4f]

Very recently, we demonstrated that [$Ru_3(CO)_{12}$] catalyzes the reaction between 1,4-diazabutadienes, CO and ethylene to

[a] Dr. habil. W. Imhof, A. Göbel, Dr. H. Görls
Institut für Anorganische und Analytische Chemie der Friedrich-Schiller-Universität Jena
August-Bebel-Strasse 2, 07743 Jena (Germany)
Fax: (+49) 3641-948102
E-mail: cwi@rz.uni-jena.de

[b] Prof. Dr. E. Anders
Institut für Organische Chemie und Makromolekulare Chemie der Friedrich-Schiller-Universität Jena
Humboldtstrasse 10, 07743 Jena (Germany)
Fax: (+49) 3641-948210
E-mail: c5eran@rz.uni-jena.de

Supporting information for this article is available on the WWW under http://www.wiley-vch.de/home/chemistry/ or from the author. It includes Table 4 with a comparison of the relative energies of all elementary steps at 0 K and 298 K (1 atm) as well as at 438 K (10 atm).

0947-6539/03/0905-1166 $ 20.00+.50/0 *Chem. Eur. J.* **2003**, *9*, No. 5

selectively produce pyrrolidin-2-one derivatives in a three-component reaction.[5] Because we used cyclic imines, we were able to obtain spirolactams from these reactions, in which regioselectively only one of the imine subunits of the starting material has been transformed.

It is widely accepted that metal-catalyzed cycloaddition reactions proceed in a stepwise fashion. There is some mechanistic evidence that the intramolecular Pauson–Khand reaction takes place via the substitution of a CO ligand by ethylene followed by the formation of a C–C bond between the alkyne and the alkene. The insertion of CO into a metal–carbon bond and the reductive elimination of the cyclopentenone completes the reaction sequence.[6] Very recently, DFT calculations on the Pauson–Khand reaction on the basis of this mechanistic evidence have been published in order to provide a deeper understanding of the regioselectivity of this reaction.[7]

Since lactones, as well as lactams, are important building blocks in a number of natural products and compounds of pharmaceutical interest,[8] we were also interested in the mechanism of this metal-catalyzed cycloaddition reaction. This knowledge will be useful in the design of new synthetic procedures towards these classes of compounds. In addition, computational techniques have proven to be powerful tools in understanding reactions of transition metal complexes by making it possible to rationalise experimental results, especially with regard to catalytic reactions.[9] Therefore, a series of high-level DFT calculations have been performed in order to calculate a complete catalytic cycle, which explains the experimentally observed formation of lactams by the three-component reaction of an diimine with CO and ethylene.

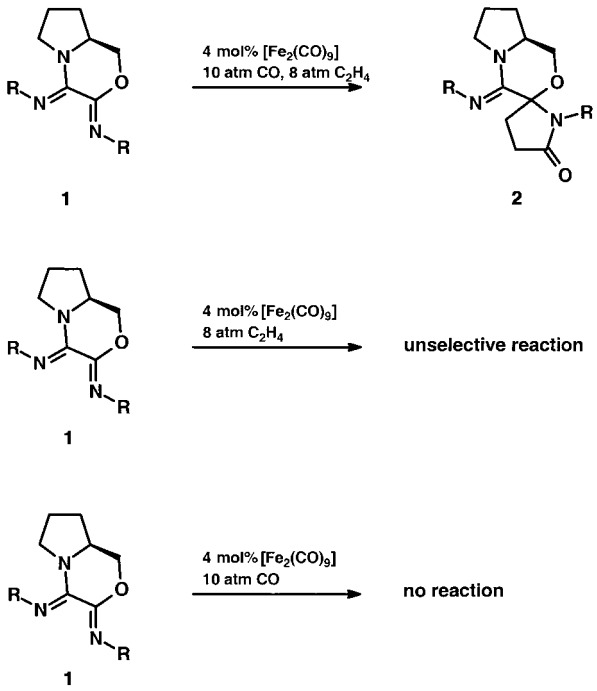

Scheme 1. Catalytic reaction of *N*,*N*′-bis-(*p*-tolyl)-tetrahydropyrrolo-[2,1c][1,4]oxazine-3,4-diylidenediamine with CO and/or ethylene.

Results and Discussions

Orientating experiments: To obtain deeper insight into the reaction course, we performed some orientating experiments. For economical as well as for toxicological reasons, we were interested whether the reaction of *N*,*N*′-bis(aryl)tetrahydropyrrolo-[2,1c][1,4]oxazine-3,4-ylidenediamines, **1**, with CO and ethylene that yields spirolactams, **2**, may be catalyzed by iron carbonyl complexes in addition to $[Ru_3(CO)_{12}]$, as some of us had previously demonstrated.[5] In general, we found that the reaction also leads to the catalytic formation of the corresponding spirolactams in the presence of $[Fe_2(CO)_9]$, although the turnover numbers and frequencies are quite low. In the presence of 4 mol % $[Fe_2(CO)_9]$, 55 % of **1** is selectively converted to **2**, while the rest remains unreacted. To find out whether the insertion of ethylene or CO is the first reaction step, we performed the catalysis with ethylene and without CO or vice versa. The results are depicted in Scheme 1: there is no reaction at all in the presence of CO without additional ethylene. In contrast, if the starting material is reacted with ethylene alone, it is consumed to the same extent as in the experiments that used mixtures of CO and ethylene. Nevertheless, the reaction is not at all selective as a large number of different compounds is produced, presumably oligomeric and polymeric compounds. These experiments led us to the conclusion that the insertion of ethylene is the first reaction step in the catalytic reaction that finally leads to the formation of pyrrolidinones.

Another important test was the reaction of an imine instead of a 1,4-diazabutadiene under the same reaction conditions as in the synthesis of the spirolactams. Again, catalysis occurs; however, it is much less selective. In our opinion, this is strong evidence that the diimine serves as a chelating ligand during catalysis.

In conclusion, we assumed that the catalytically active species should be a mononuclear iron carbonyl complex with the iron atom coordinated by the 1,4-diazabutadiene in a chelating manner. This seems to be reasonable because it has been shown by DFT calculations that $[Fe_2(CO)_9]$ will decompose to yield mononuclear fragments at the temperatures that we used for the catalytic reactions.[10] These mononuclear fragments may react with a diazabutadiene substrate to build a complex of the general formula [(1,4-diaza-butadiene)Fe-$(CO)_3$].

Test of the B3LYP/6-311++G(d,p) method: (For computational details, see the Experimental Section). Although the coordination chemistry of diazabutadiene ligands coordinated to iron and ruthenium centres has been extensively studied during the past decades,[11] to our surprise, only one mononuclear [(diazabutadiene)Fe$(CO)_3$] complex has been characterized by X-ray crystallography.[12] In some cases, such complexes have been proposed to be the intermediates in the formation of diazabutadiene metal carbonyls of higher nuclearity.[13]

During our studies on the chemistry of glyoxal-bisimines, we were able to isolate a mononuclear iron carbonyl complex which was also characterized by an X-ray structure analysis. The molecular structure of (glyoxaldiylidene-bis-4-methox-

  0947-6539/03/0905-1167 $ 20.00+.50/0

yaniline)irontricarbonyl (**3**) is shown in Figure 1. The same molecule was calculated with the level of theory we decided to use for the calculation of the intermediates and transition states of the catalytic cycle. The most important bond lengths, bond angles and torsional angels from the X-ray structure analysis and from the calculations are summarized in Table 1.

The comparison of the data shows that the B3LYP-/6-311++G(d,p) level leads to an excellent agreement of the outcome of the calculations and the structural analysis. The values calculated for bond lengths and angles of **3** are mostly in the range of the standard deviations of the structure analysis. The X-ray structure determination shows a square-pyramidal coordination sphere around iron with a crystallographic mirror plane through iron, the apical CO ligand and the centre of the C–C bond between the imine carbon atoms of the diazabutadiene ligand. The bond lengths and bond angles are in the expected range, particularly those of the diazabutadiene system. The imine double bonds are lengthened as a result of coordination of the nitrogen atoms, whereas the central C–C bond is shortened. Similar trends were observed for the other [(diazabutadiene)-$Fe(CO)_3$] complex characterized by X-ray crystallography.[12] Together with the fact that **3** as well as other 1,4-diazabutadiene compounds are diamagnetic iron or ruthenium low-spin complexes,[11] the comparison of the calculated structure with the experimentally determined bond lengths and angles show that the level of theory used herein is suitable to handle the calculations of stationary points of the catalysis.

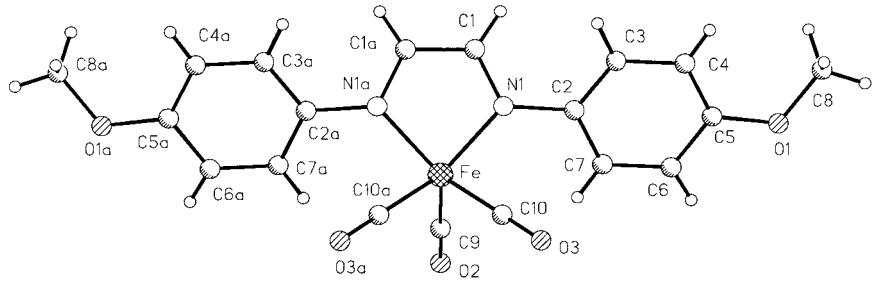

Figure 1. The molecular structure of **3**.

Table 1. Bond lengths [pm], angles [°], and torsional angles [°] of **3** (B3LYP/6-311++G(d,p) results are given in italics).

Fe–N1	194.2(2), *194.9*	Fe–C9	180.1(4), *178.5*	Fe–C10	178.9(3), *181.2*
N1–C1	134.2(3), *133.8*	N1–C2	143.9(3), *142.6*	C1–C1a	139.0(5), *138.8*
C2–C3	139.1(3), *139.6*	C3–C4	139.7(3), *139.6*	C4–C5	138.9(3), *139.6*
C5–C6	138.9(3), *140.0*	C6–C7	139.0(3), *138.5*	C7–C2	139.7(3), *140.2*
C5–O1	137.8(3), *136.4*	O1–C8	143.8(5), *142.1*	C9–O2	115.5(4), *114.8*
C10–O3	115.6(4), *114.5*				
C10-Fe-C10a	87.3(1), *87.7*	C10-Fe-C9	99.1(1), *99.4*	C10-Fe-N1	90.45(9), *90.5*
N1-Fe-N1a	81.1(1), *80.9*	N1-C1-C1a	115.0(1), *115.2*	C3-C2-N1	121.7(2), *120.8*
C4-C3-C2	120.9(2), *121.2*	C5-C4-C3	119.5(2), *119.8*	C6-C5-C4	120.0(2), *119.3*
C7-C6-C5	120.2(2), *120.5*	C2-C7-C6	120.4(2), *120.7*	C7-C2-N1	119.4(2), *120.7*
O1-C5-C4	124.5(3), *124.7*	O1-C5-C6	115.5(3), *115.9*	C8-O1-C5	118.0(4), *118.6*
Fe-C9-O2	179.8(4), *179.1*	Fe-C10-O3	178.3(4), *178.3*		

Calculations on the mechanism of the catalytic cycloaddition reaction: Figures 2 and 3 show the intermediates and transition states as well as the energy

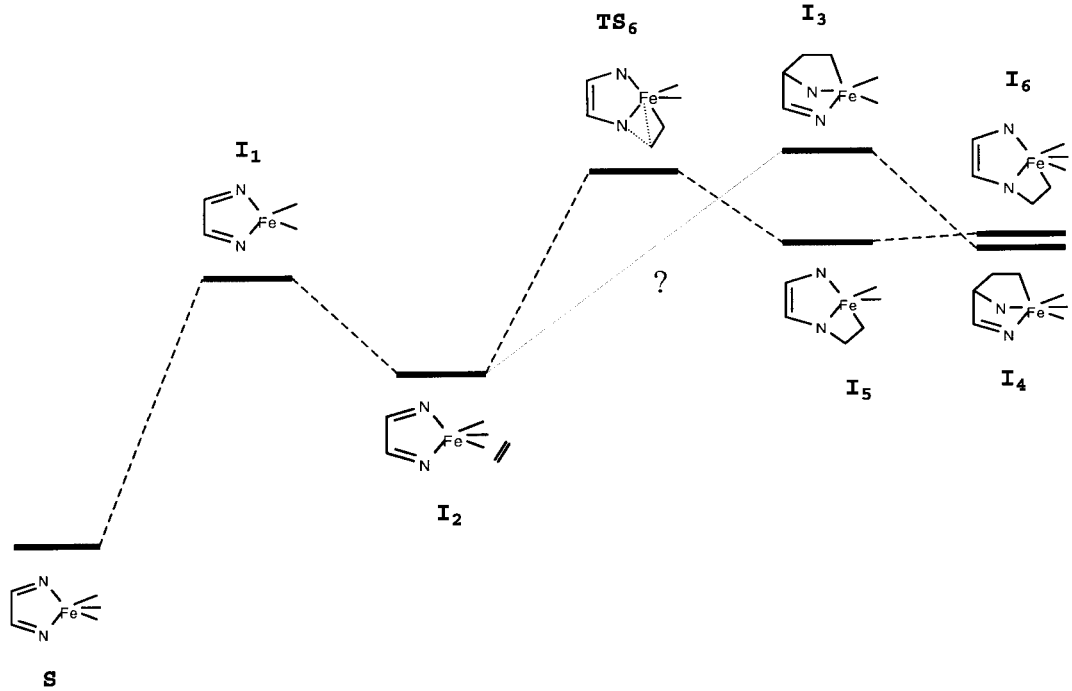

Figure 2. The addition of ethylene to **S** by a dissociative/interchange pathway. For relative free energies of the starting complex **S**, $\mathbf{TS_6}$ and the intermediates $\mathbf{I_1}$–$\mathbf{I_6}$, see Table 3.

0947-6539/03/0905-1168 $ 20.00+.50/0 *Chem. Eur. J.* **2003**, *9*, No. 5

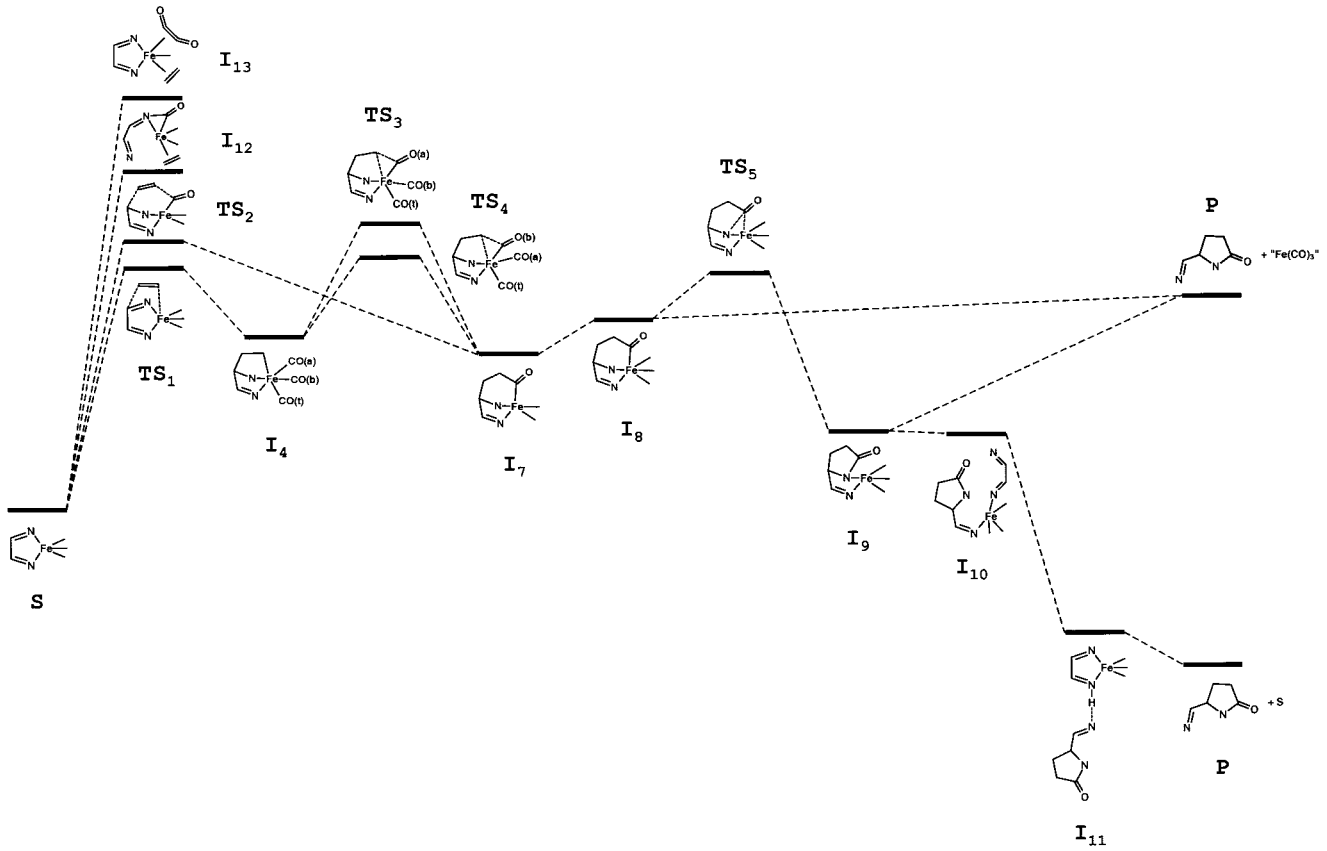

Figure 3. The interaction of ethylene with **S** by an associative pathway and the formation of the product compound **P**. For relative free energies of the starting compound **S**, the transition states $\mathbf{TS_1}-\mathbf{TS_5}$, the intermediates $\mathbf{I_4}$ and $\mathbf{I_7}-\mathbf{I_{13}}$ and **P**, see Table 3.

differences between them calculated by the B3LYP/6-311++G(d,p) method. Table 2 summarises the DFT (B3LYP) total energies E for all stationary points calculated with LANL2DZ and the 6-311++G(d,p) basis sets. As bimolecular reactions are involved (such as $\mathbf{S} + C_2H_4 \rightarrow \mathbf{I_4}$), we calculated thermal and entropic corrections under standard reaction conditions (298.5 K, 1 atm).[14, 15] The resulting values E_{corr} (Table 2) and in addition, the relative Gibbs free energies ΔG for the elementary steps (Table 3) allow a more realistic estimate of the intrinsic relative energy relationships than those resulting from the relative E values. In addition, some of the key intermediates and transition states have also been calculated with the standard augmented correlation-consistent triple ζ basis set with a relativistic ECP of the SD group in conjunction with the [2f,1g] set. The comparison of the equilibrium geometries calculated with the B3LYP/aug-cc-pVTZ and the B3LYP/6-311++G(d,p) procedures reveals acceptable agreement, again showing that the latter is suitable to calculate the stationary points of the catalytic cycloaddition reaction we are interested in. Table 3 lists the elementary steps and their relative free energies compared to the starting complex **S**. Figures 4–7 show the calculated molecular structures of the starting compound **S**, all intermediates and transition states as well as the final product **P** together with the some selected bond lengths.

We knew from several experiments (vide supra) that the first step of the catalytic cycle is the reaction of ethylene with the coordinated diazabutadiene. As a starting complex, we chose **S**, which is a [(1,4-diaza-butadiene)$Fe(CO)_3$] complex that is comparable with **3** on account of the identical ligand environment of the central iron atom. The organic substituents at the imine nitrogen atoms have been replaced by hydrogen. A comparison of the calculations of **S** (Figure 4) with the structure determination of **3** (Figure 1) reveal essentially identical structural properties with regard to bond lengths and angles as well as the symmetry properties of the complex. The slight differences in the bond lengths of the apical and equatorial CO ligands may be caused by packing effects in the structure determination of **3**, since CO ligands act as acceptors of hydrogen bonds in crystalline compounds.[16] In addition, charge densities and bond orders and thus the electronic properties of **3** and **S** are essentially the same showing that **S** is an acceptable model for **3**.

It is well-accepted for a wide variety of transition metal-catalyzed reactions that a catalytic cycloaddition reaction starting from **S** should proceed by the formal substitution of one CO ligand by ethylene ($\mathbf{I_2}$), which then would undergo subsequent reactions and thus form the observed products. It has been shown by computational methods that CO-substitution reactions in $[Fe(CO)_5]$ and in 18-electron complexes, in general, follow a dissociative or a dissociative/interchange mechanism.[17] Therefore, we first investigated the dissociation of a CO ligand from the starting compound **S**. The results are depicted in Scheme 2. Because **S** is a complex with a square-pyramidal geometry, there are two different types of CO ligands. If the bond length between an equatorial ligand

  0947-6539/03/0905-1169 $ 20.00+.50/0

Table 2. Calculated total energies (E) and energies after thermal and entropic corrections (E_{corr}) at 298.5 K and 1 atm for ethylene, carbon monoxide, 1,4-diazabutadiene (s-*cis* conformation), [Fe(CO)$_3$], **S**, **I$_1$**–**I$_{13}$**, **TS$_1$**–**TS$_7$** and **P**.

Compound	B3LYP/LANL2DZ			B3LYP/6-311++G(d,p)			B3LYP/6-311++G(d,p)
	$-E$ [a.u.]	Nimag[a]	ZPE [kcal mol^{-1}]	$-E$ [a.u.]	Nimag[a]	ZPE [kcal mol^{-1}]	$-E_{corr}$ [a.u.]
C_2H_4	78.5782089	[0]	32.21	78.6155382	[0]	31.87	78.586283
CO	113.2778564	[0]	2.9	113.3490503	[0]	3.16	113.363132
$C_2H_4N_2$ (one N-H–N)	188.0298001	[0]	39.15	188.1313986	[0]	39.23	188.0956406
$C_2H_4N_2$ (no N-H–N)	188.022714	[0]	38.99	188.1283669	[0]	39.14	188.092700
[Fe(CO)$_3$]				1603.7874649	[0]	15.10	1603.796751
S	651.5143798	[0]	57.94	1792.0467359	[0]	57.84	1791.992897
I$_1$	538.1615878	[0]	52.08	1678.6334392	[0]	51.87	1678.586080
I$_2$	616.7779717	[0]	86.88	1757.2877968	[0]	86.50	1757.188242
I$_3$	616.7451664	[0]	88.20	1757.2550047	[0]	87.82	1757.151592
I$_4$	730.0687745	[0]	93.24	1870.6396917	[0]	93.09	1870.530783
I$_5$	616.7645287	[0]	88.27	1757.2695701	[0]	87.87	1757.166748
I$_6$	730.0700104	[0]	93.15	1870.6359125	[0]	92.65	1870.528677
I$_7$	730.0862129	[0]	94.73	1870.6470717	[0]	94.34	1870.535962
I$_{7T}$	730.0542567	[0]	93.06	1870.6157514	[0]	92.72	
I$_8$	843.3844718	[0]	99.29	1984.0051137	[0]	99.12	1983.889600
I$_9$	843.4225691	[0]	100.94	1984.0357842	[0]	100.33	1983.921341
I$_{10}$				2172.186819	[0]	140.88	2172.014860
I$_{11}$				2172.241075	[0]	141.54	2172.070449
I$_{12}$	730.0285667	[0]	91.13	1870.588991	[1]	90.85	1870.484242
I$_{13}$	730.0099235	[0]	91.70	1870.5688762	[0]	91.47	1870.463678
TS$_1$	730.0465156	[1]	91.17	1870.615980	[1]	90.93	1870.511230
TS$_2$	730.0442949	[1]	91.83	1870.609582	[1]	91.67	1870.503750
TS$_3$				1870.6074719	[1]	92.48	1870.499063
TS$_4$				1870.6177348	[1]	92.80	1870.508539
TS$_5$				1983.9917928	[1]	98.60	1983.876458
TS$_6$				1757.2552063	[1]	86.42	1757.154971
TS$_7$				1757.2189212	[1]	86.13	1757.118471
P	380.0079748	[0]	83.53	380.1866035	[0]	82.87	380.086717

[a] *N*umber of *imag*inary frequencies. [b] B3LYP/aug-cc-pVTZ optimizations: C_2H_4: 78.6240647, 0, 31.93; $C_2H_4N_2$ (no N-H–N): 188.1467133, 0, 39.13; **S**: 652.305576, 0, 57.89; **I$_9$**: 844.3100810;[c] **TS$_1$**: 730.8829459;[c] **TS$_2$**: 730.8760423;[c] **TS$_4$**: 730.8838839;[c] **P**: 380.2211039, 0, 82.90. [c] Frequency calculations have not been performed.

Table 3. Relative Gibbs free energies of all elementary steps leading to **I$_1$**–**I$_{13}$**, **TS$_1$**–**TS$_7$** and **P**.

Elementary step	ΔG[a] [kcal mol^{-1}]	Elementary step	ΔG[a] [kcal mol^{-1}]
S → **I$_1$** + CO	27.4	**I$_4$** → **TS$_3$**	19.9
I$_1$ + C_2H_4 → **I$_2$**	−10.0	**I$_4$** → **TS$_4$**	14.0
I$_2$ → **I$_3$**	23.0	**TS$_2$** → **I$_7$**	−20.2
I$_3$ → **TS$_7$**	20.8	**TS$_3$** → **I$_7$**	−23.2
I$_2$ → **I$_5$**	13.5	**TS$_4$** → **I$_7$**	−17.2
I$_2$ → **TS$_6$**	20.9	**I$_7$** + CO → **I$_8$**	6.0
TS$_6$ → **I$_5$**	−7.4	**I$_8$** → **TS$_5$**	8.2
I$_3$ + CO → **I$_4$**	−10.1	**TS$_5$** → **I$_9$**	−28.2
I$_5$ + CO → **I$_6$**	0.8	**I$_9$** + $C_2H_4N_2$ → **I$_{10}$**	−0.5
S + C_2H_4 → **TS$_1$**	42.6	**I$_8$** → **P** + [Fe(CO)$_3$]	3.9
S + C_2H_4 → **TS$_2$**	47.3	**I$_9$** → **P** + [Fe(CO)$_3$]	23.8
S + C_2H_4 → **I$_{12}$**	59.6	**I$_{10}$** → **I$_{11}$**	−34.9
S + C_2H_4 → **I$_{13}$**	72.5	**I$_{11}$** → **P** + **S**	−5.8
TS$_1$ → **I$_4$**	−12.3		

[a] Values have been determined taking frequency calculations into consideration.

and the iron centre is increased stepwise, it finally dissociates from **S** to generate the intermediate **I$_1$** (Figure 2 and Scheme 2). If the same procedure is applied to the axial CO ligand, a pseudo-rotation takes place transforming the former axial CO group into an equatorial one, and an equatorial CO ligand of **S** migrates towards the axial position from which it disappears again to generate **I$_1$**. This pseudo-rotation may also be rationalized by the fact that in a MO diagram of a square-pyramidal complex, the xy, xz and yz orbitals, which are non-bonding orbitals, are responsible for the backdonation of electron density from the metal into the π* orbital of the CO ligands. This backdonation is most effective for the ligand in axial position and, therefore, the dissociation of the equatorial CO is the less energetic process. Thus, if the bond length of the axial ligand is increased to a Fe–C bond length of ≈2.368 Å, the system helps itself by interchanging the ligands by a pseudo-rotation to convert the axial ligand to an equatorial one which might then be eliminated more readily.

The molecular structure of **S** and **I$_1$**, calculated with the B3LYP/6-311++G(d,p) method, are shown in Figure 4. As already indicated, the bond lengths and angles of **S** correspond very well with those calculated for **3**. According to the loss of an equatorial CO ligand, the C–Fe bond length of the axial CO group in **I$_1$** is shortened by 2.4 pm compared to **S**. In addition, the N–Fe bond *trans* to the free coordination site in **I$_1$** is 5.1 pm shorter than that in the starting compound; this corresponds to an increased bond strength. The remaining bond lengths are almost not affected by the elimination of an CO ligand in **S** to produce **I$_1$**. This reaction that generates **I$_1$** is endothermic by 27.4 kcal mol^{-1}. As expected, the electronically unsaturated compound **I$_1$** is significantly less stable than the starting complex **S** (Figure 2, Table 3).

The addition of ethylene to **I$_1$** leads to an 18-electron iron complex **I$_2$**. The reaction is exothermic by 10.0 kcal mol^{-1}

0947-6539/03/0905-1170 $ 20.00+.50/0 *Chem. Eur. J.* **2003**, *9*, No. 5

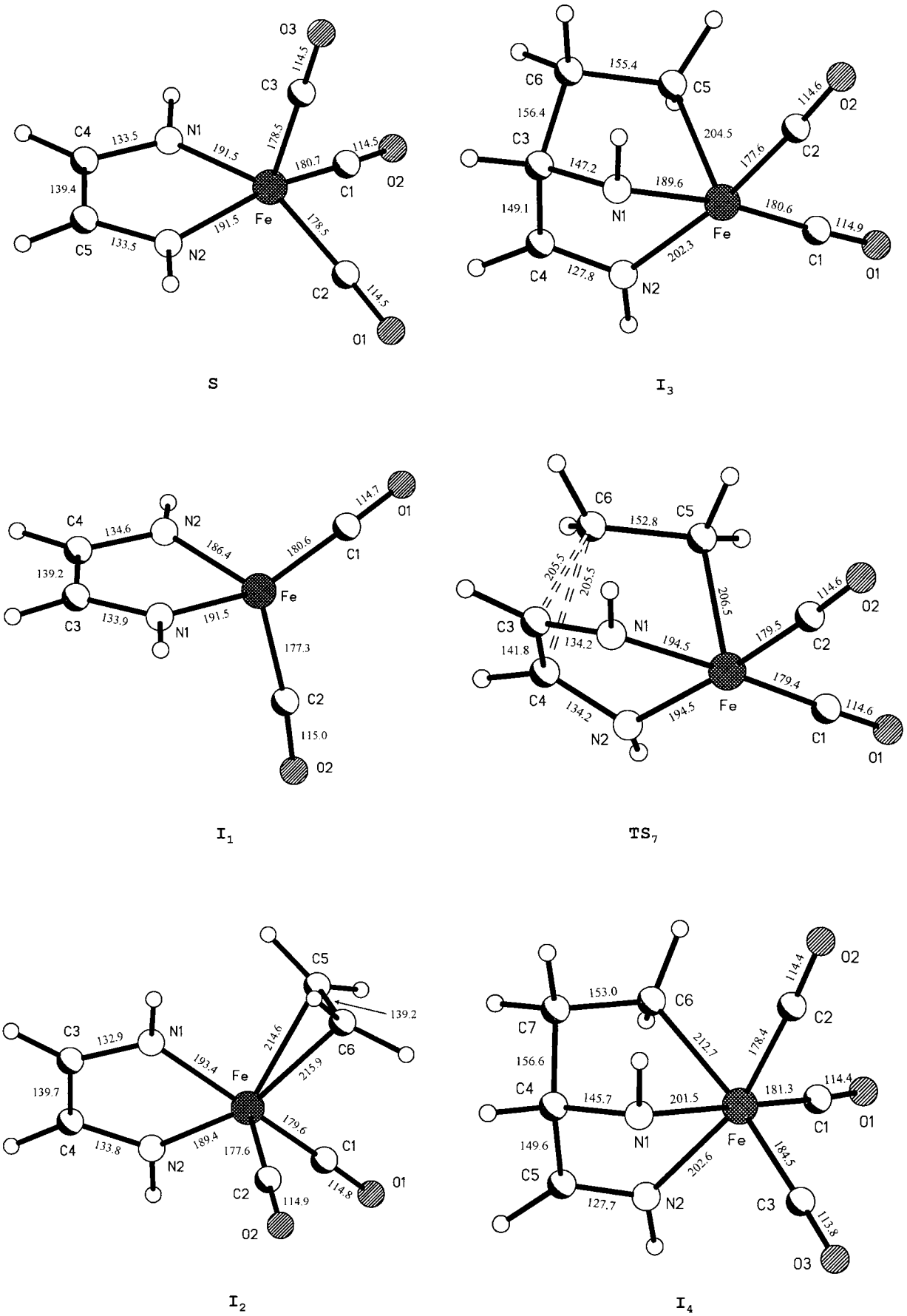

Figure 4. Structures of **S**, **I**$_1$–**I**$_4$ and **TS**$_7$ optimized at the B3LYP/6-311++G(d,p) level, distances given in pm.

  0947-6539/03/0905-1171 $ 20.00+.50/0

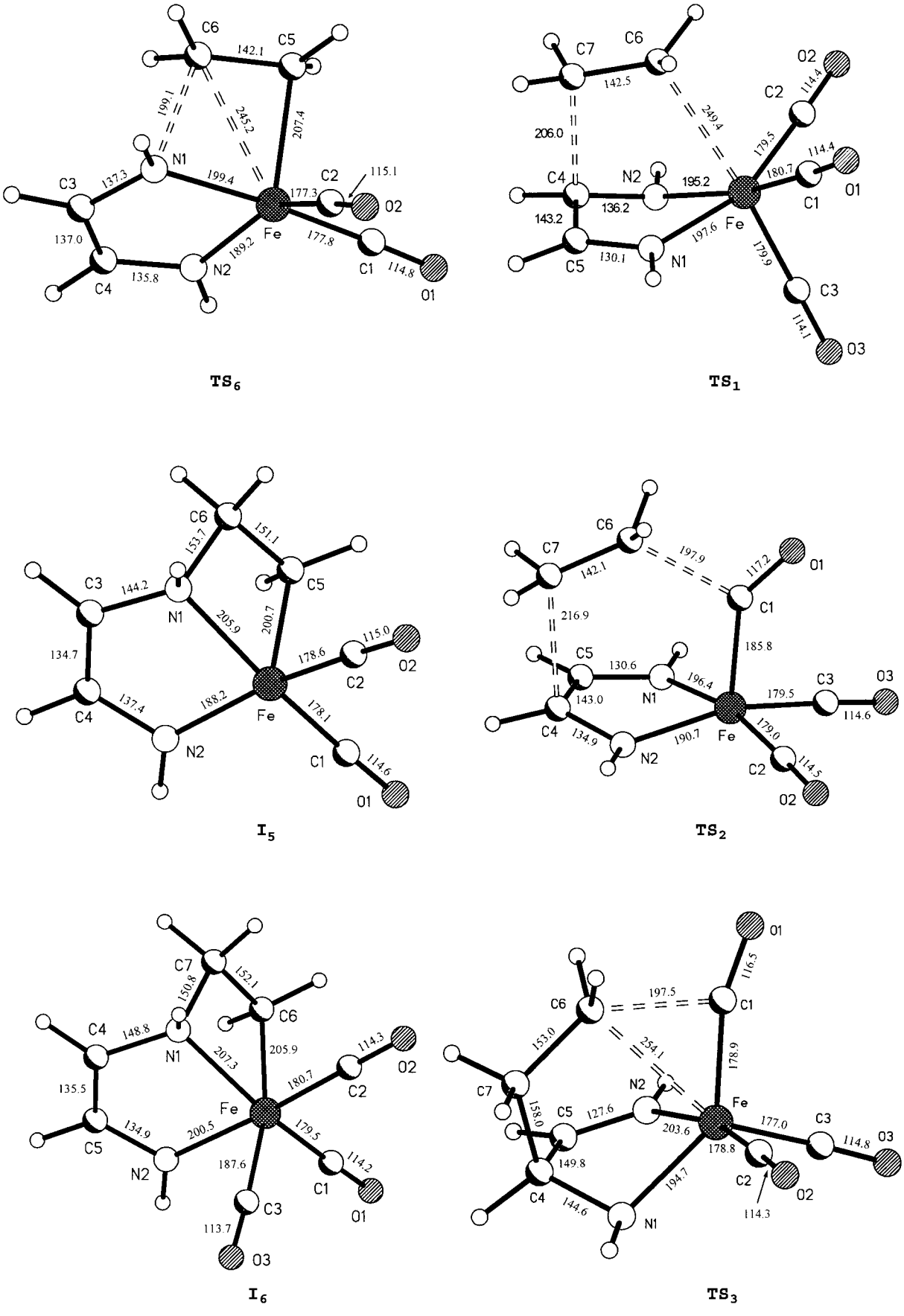

Figure 5. Structures of $\mathbf{TS_1}$–$\mathbf{TS_3}$, $\mathbf{TS_6}$, $\mathbf{I_5}$ and $\mathbf{I_6}$ optimized at the B3LYP/6-311++G(d,p) level, distances given in pm.

0947-6539/03/0905-1172 $ 20.00+.50/0 *Chem. Eur. J.* **2003**, *9*, No. 5

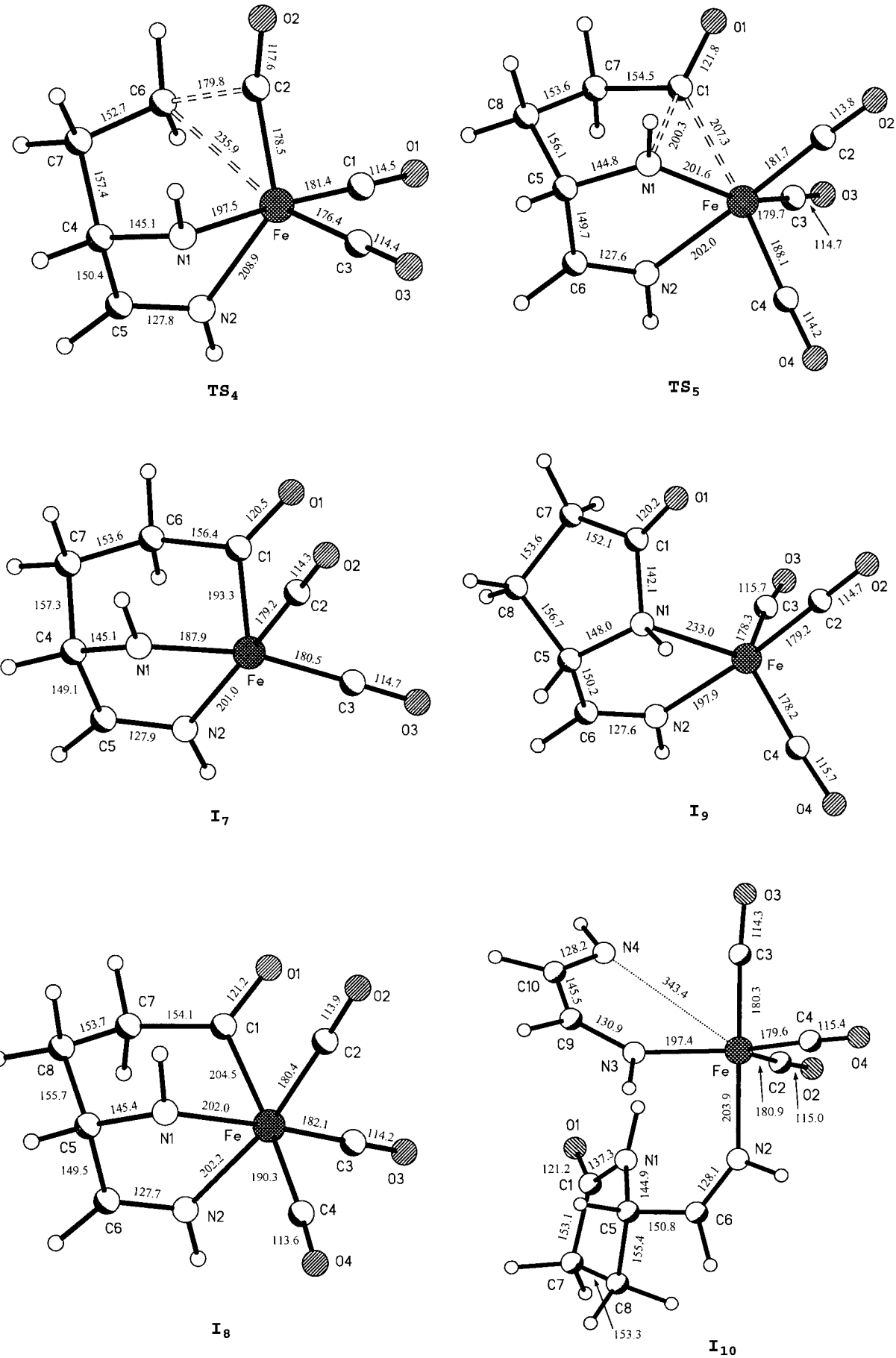

Figure 6. Structures of $\mathbf{I_7}$–$\mathbf{I_{10}}$, $\mathbf{TS_4}$ and $\mathbf{TS_5}$ optimized at the B3LYP/6-311++G(d,p) level, distances given in pm.

  0947-6539/03/0905-1173 $ 20.00+.50/0

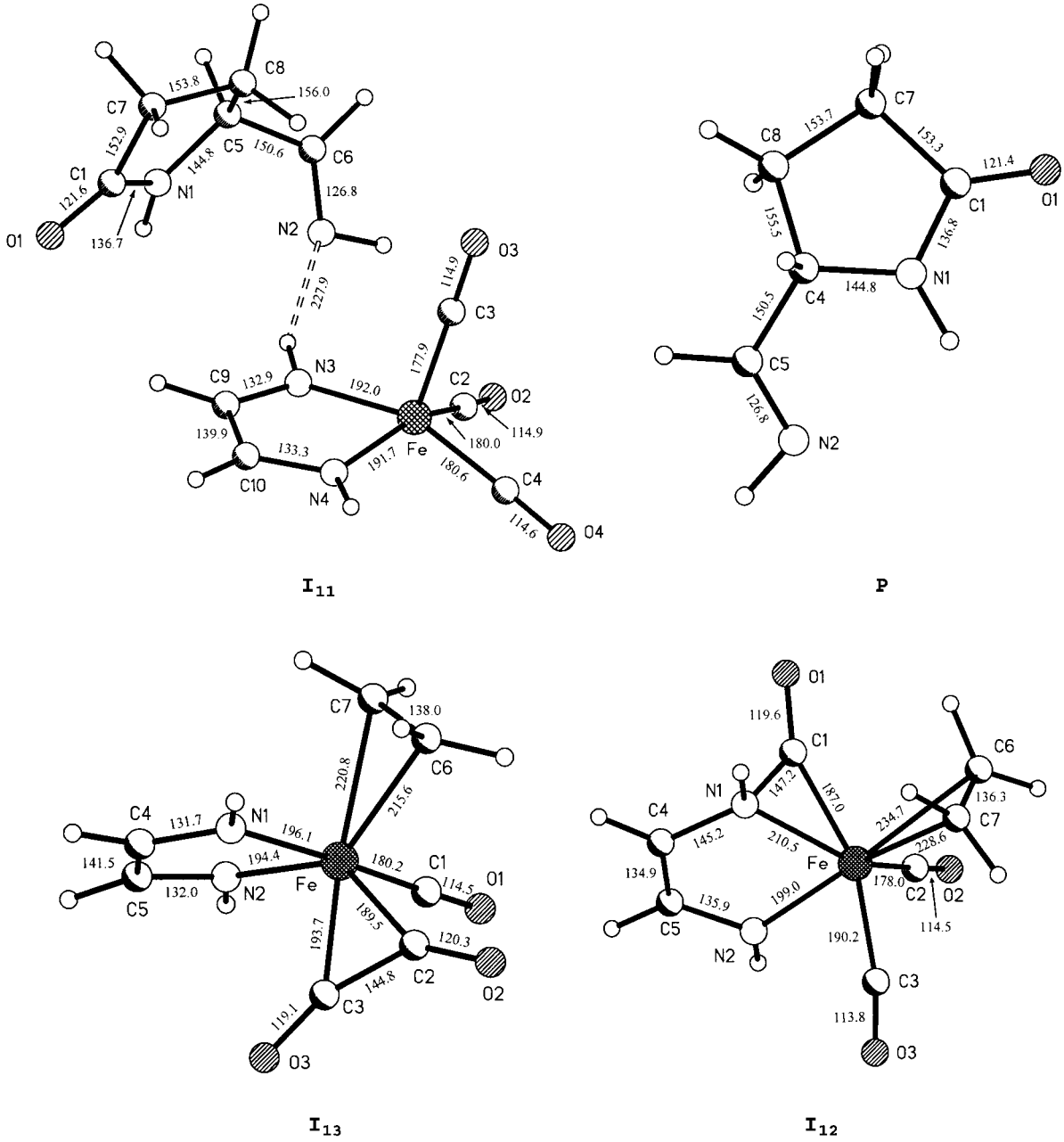

Figure 7. Structures of $\mathbf{I_{11}}$–$\mathbf{I_{13}}$ and **P** optimized at the B3LYP/6-311++G(d,p) level, distances given in pm.

(Figure 2, Table 3). The coordination mode of iron in $\mathbf{I_2}$ is trigonal-bipyramidal with the ethylene ligand in an equatorial position (Figure 4). This corresponds very well with the molecular structures of the few iron ethylene complexes which were characterized by X-ray diffraction.[18] The structure is also very similar to $[CpRu(\eta^2\text{-}C_2H_4)(1,4\text{-diazabutadiene}]^+$, which was described by Vrieze et al.[19] The axial positions are occupied by one of the CO ligands (C1–O1) and one nitrogen atom of the diazabutadiene ligand (N1). The bond lengths and angles are in the range of expected values. The bonds between iron and the axial ligands are elongated compared to the same coordination sites in equatorial positions. The ethylene ligand is bound in a symmetrical fashion, which indicates that the Fe–C bond lengths are nearly identical (214.6 and 215.9 pm).

The interaction of the ethylene ligand coordinated side-on in $\mathbf{I_2}$ with the diazabutadiene ligand may, in principle, proceed by two different reaction pathways.

Pathway 1: Formation of a C–C bond between ethylene and one of the imine carbon atoms (C3) of the diazabutadiene ligand to generate $\mathbf{I_3}$ (Figures 2 and 4), which is an endothermic process (23.0 kcal mol^{-1}, Table 3). This pathway does not appear to be very realistic, as in $\mathbf{I_2}$ the shortest distance $C_{ethylene}$–C3 is 395.5 pm. Despite many attempts, we never succeeded in locating a transition structure that connects $\mathbf{I_2}$ and $\mathbf{I_3}$. Nevertheless, it is hard to tell for certain whether this pathway can be excluded. $\mathbf{I_3}$ is an iron(II) complex of square-pyramidal geometry, in which the diazabutadiene and ethylene generate a formally dianionic tridentate ligand. Accord-

0947-6539/03/0905-1174 $ 20.00+.50/0 *Chem. Eur. J.* **2003**, *9*, No. 5

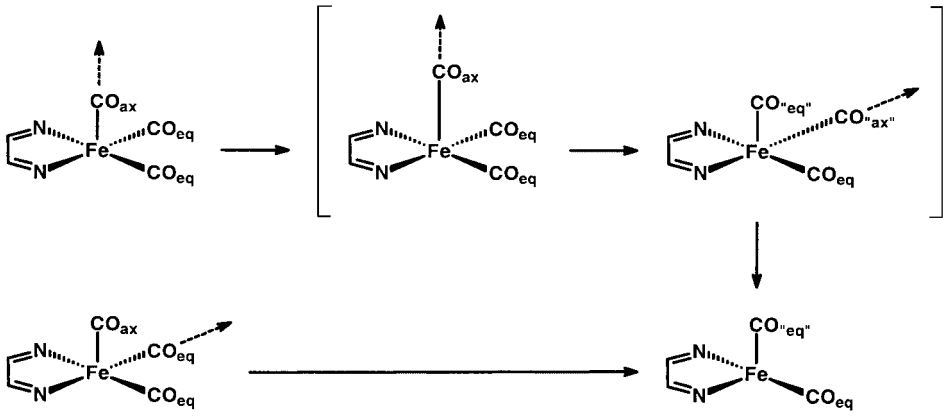

Scheme 2. Dissociation of a terminal CO ligand of **S** from an equatorial or from the apical position.

ing to this interpretation, the bond between the imine nitrogen atom N2 and iron is 12.7 pm longer than the bond between the amide nitrogen (N1) and iron. Correspondingly, the bond length of the CO ligand *trans* with respect to the imine nitrogen (N2) is 3.0 pm shorter than the bond between iron and the CO group *trans* with respect to the amide nitrogen. Furthermore, the length of the bond between C3 and the amide nitrogen N1 is indicative of a single bond (147.2 pm), whereas the bond between N2 and C4 is shortened ($\mathbf{I_3}$: 127.8 pm, $\mathbf{I_2}$: 133.8 pm) because now there is no conjugation to another imine double bond. The other bond lengths and angles are in the expected ranges.

In the course of our systematic investigations, we located a transition structure $\mathbf{TS_7}$ (Figure 4) which determines the interconnecting pathway between the ethylene carbon atom being bound to the equivalent imine carbon atoms of the diazabutadiene moiety (c.f. $\mathbf{I_3}$). This transition state shows a perfect symmetry with respect to a plane through Fe, C5 and the centroid of the C3–C4 bond. In the case of our simplified model compounds, the resulting activation barrier is 20.8 kcal mol^{-1}. This value should be a function of the substitution pattern at the C and N atoms of the diazabutadiene ligand.

Since $\mathbf{I_3}$ is a 16-electron complex, the addition of another CO ligand leads to the coordinatively saturated octahedral complex $\mathbf{I_4}$ (Figures 2 and 4). The reaction is exothermic by 10.1 kcal mol^{-1} (Table 3). The formation of an 18-electron complex has some influence on the bonding of the dianionic tridentate ligand formed from the diazabutadiene and ethylene towards iron. The C6–Fe bond length in the *trans* position with respect to the new CO ligand is increased by 8.2 pm compared to the situation in $\mathbf{I_3}$. In addition, the N1–Fe bond is elongated by 11.9 pm, whereas the other bond lengths and angles are almost unaffected. The observed changes in the bonding of the dianionic moiety to the metal centre reflect the situation of the iron atom in $\mathbf{I_4}$ now being electronically saturated and so the bonding to the most nucleophilic centres of the ligand environment is weaker than in $\mathbf{I_3}$. In summary, the formation of $\mathbf{I_3}$ and $\mathbf{I_4}$, respectively, would lead to a new C–C bond between the ethylene ligand and one of the imine carbon atoms of the former diazabutadiene ligand which is also observed in the products, such as **2**, obtained in the experiments (Scheme 1).

Pathway 2: A reaction channel in which a bond between ethylene and one of the imine nitrogen atoms (N1) is formed to produce $\mathbf{I_5}$ via $\mathbf{TS_6}$ seems to be more reasonable for steric reasons (Figures 2 and 5). The $C_{ethylene}$–N_{axial} distance in $\mathbf{I_2}$ is 286.4 pm, which shortens to 199.1 pm in $\mathbf{TS_6}$. The activation barrier for this process is 20.9 kcal mol^{-1}. In $\mathbf{TS_6}$, the trigonal-bipyramidal coordination sphere around iron is preserved to a great extent, although one of the ethylene carbon atoms (C5) is moved in the direction of N1. The bond lengths between N1 and iron or C3 are elongated compared to $\mathbf{I_2}$ as a result of the interaction with C5. Thus, in contrast to pathway 1 ($\mathbf{I_2} \rightarrow \mathbf{I_3}$), the intramolecular formation of $\mathbf{I_5}$ from $\mathbf{I_2}$ via $\mathbf{TS_6}$ should be feasible as well as the back-reaction, for which a barrier of only 7.4 kcal mol^{-1} has to be surmounted.

It is noteworthy that the formation of $\mathbf{I_5}$ is energetically favored by 9.5 kcal mol^{-1} compared to $\mathbf{I_3}$ (Table 3). $\mathbf{I_5}$ shows a highly distorted trigonal bipyramidal coordination sphere around iron. The formation of a C–N bond generates a four-membered ring (Fe-C5-C6-N1), which is responsible for the observed distortion of the trigonal-bipyramidal coordination sphere, and which may also be responsible for the low activation barrier to recover $\mathbf{I_2}$. The calculated bond lengths correspond to the description of $\mathbf{I_5}$ as a 16-electron iron(II) complex. N1 now represents an amine nitrogen atom that is coordinated to the iron centre by its lone pair. So the N1–C3 bond is in the range of a single bond (144.2 pm), whereas the bond between the two imine carbon atoms of the former diazabutadiene ligand (C3 – C4) shows a value typical for C–C double bonds (134.7 pm). The second nitrogen atom N2 is negatively charged, thus leading to a nitrogen – iron bond (188.2 pm) shorter than the N1–Fe bond (205.9 pm).

Addition of CO to the 16-electron species $\mathbf{I_5}$ results in the formation of the 18-electron complex $\mathbf{I_6}$ (Figures 2 and 5). This reaction is endothermic by 0.8 kcal mol^{-1} (Table 3) for entropic reasons in combination with the highly strained four-membered ring system. The latter is also responsible for the distorted octahedral coordination around iron in $\mathbf{I_6}$. Again, the fact that iron now is electronically saturated leads to a lengthening of the bonds between the formally anionic centres N2 and C6 and iron compared to the situation in $\mathbf{I_5}$. The other bond lengths and angles are almost unaffected by the addition of a third CO ligand.

There are systems described in the literature which may serve as models for the above-mentioned reactions. Iron or ruthenium 1,4-diazabutadiene complexes react with alkynes to produce organometallic compounds in which a new C–N bond or a new C–C bond, respectively, between the alkyne and the diazabutadiene ligand has been formed. This would correspond to the formation of $\mathbf{I_5}$ or $\mathbf{I_6}$. On the other hand, depending on the reaction conditions and the alkyne properties, the reaction may also lead to a system in which the

  0947-6539/03/0905-1175 $ 20.00+.50/0

diazabutadiene, the alkyne and one CO ligand are coupled.[20] The reaction of [(1,4-diazabutadiene)$Fe(CO)_3$] complexes with alkenes does not lead to isolable products. Nevertheless, if all CO ligands are exchanged by bulky isonitrile moieties, an equilibrium between the starting compounds and a complex closely related to $\mathbf{I_4}$ may be observed by NMR techniques.[18f]

As depicted in Figure 2, the formation of a C–N bond between ethylene and the diazabutadiene, leading to the formation of $\mathbf{I_5}$ and $\mathbf{I_6}$, is the energetically more favored reaction pathway compared to the alternative formation of a C–C bond to generate $\mathbf{I_3}$ and $\mathbf{I_4}$. As already indicated, we have not been able to identify any minimum reaction pathways which connect $\mathbf{I_2}$ with $\mathbf{I_3}$ or $\mathbf{I_5}$ with $\mathbf{I_3}$. In all cases, any reaction ends in the formation of $\mathbf{I_5}$ or the reformation of $\mathbf{I_2}$. For example, the stepwise elongation of the C–N bond in $\mathbf{I_5}$ always led to $\mathbf{I_2}$. In addition, we must point out that, in the course of our experimental investigations, we never detected products which would result from an intermediate, such as $\mathbf{I_6}$, as the experiments only generate products in which ethylene is connected to the former imine carbon atom. Furthermore, for the real catalytic cycle (at $\approx$440 K and elevated pressure) the formation of $\mathbf{I_5}$ and $\mathbf{I_6}$ should be strongly disfavored also from an experimental point of view on account of the steric demands of the aromatic substituents on the imine nitrogen atoms compared to that of the model substituents (the imine hydrogen atoms). Therefore, we concluded that alternative reaction channels had to be taken into account in which the ethylene molecule interacts directly with **S** without a preceding dissociation of a CO ligand. We will demonstrate in the following that these concerted reaction pathways readily explain the formation of the experimentally observed product species.

Because the starting material **S** shows a square-pyramidal geometry, the iron centre should be directly accessible from the base of the complex. If ethylene is calculated to approach stepwise towards the iron atom, the intermediate $\mathbf{I_4}$ is generated in a *concerted reaction*. The outcome of this reaction pathway is independent of the starting orientation of ethylene relative to the coordinated diazabutadiene. Thus, a reaction coordinate leading to $\mathbf{I_6}$ is *never* observed from the approach of ethylene toward the base of the square-pyramidal complex **S**. Figures 3 and 5 show the transition state $\mathbf{TS_1}$ for the formation of $\mathbf{I_4}$. The activation energy was calculated to be 42.6 kcal mol^{-1} (Table 3). As we did not detect the transition state leading to $\mathbf{I_1}$ from **S** in the calculations, there is no way of directly comparing these two initial steps of the potential catalytic cycle. Nevertheless, it is a convincing fact that the associative pathway leading to $\mathbf{I_4}$ via $\mathbf{TS_1}$ produces a C–C bond in the exact same position as it is observed in the experimental work. The activation energy of 42.6 kcal mol^{-1} is mostly probably the result of the highly negative activation entropy of this associative process. However, because the experimental results were obtained at $\approx$440 K and an ethylene and CO pressure of 10 atm, we are sure that is possible to surmount this high barrier and that an associative pathway is feasible.

The structure of $\mathbf{TS_1}$ shows that the coordination sphere around iron is changed from square pyramidal in **S** towards an octahedral arrangement by the approach of the alkene. In addition, the bond lengths of the imine moiety are strongly influenced by this process, which indicates the beginning of the interaction with ethylene. One of the imine double bonds (C4–N1) is elongated by 2.7 pm, whereas the C–C bond length of the diazabutadiene (C4–C5) is increased by 3.8 pm compared to **S**. In contrast to the starting complex **S**, the diazabutadiene ligand in $\mathbf{TS_1}$ also shows an angle of 22.9° between the diazabutadiene plane and the plane through iron and both the imine nitrogen atoms, whereas this arrangement is absolutely planar in **S**. The structure of $\mathbf{I_4}$ is, of course, identical if it is generated from $\mathbf{TS_1}$ or by the dissociative reaction pathway described above.

The stepwise approach of ethylene towards **S** from the base of the square-pyramid, as an alternative to the formation of $\mathbf{I_4}$, leads to two additional products, $\mathbf{I_{12}}$ and $\mathbf{I_{13}}$, although these reactions are much less favorable on account of their energetic demands (Figure 2, Table 3). $\mathbf{I_{12}}$ is produced in an endothermic reaction affording 59.6 kcal mol^{-1} (Table 3). The structure of $\mathbf{I_{12}}$ is shown in Figure 7. The approach of ethylene leads to a side-on coordination of the olefin. This forces one of the CO ligands to interact with one of the imine nitrogen atoms. The structure may best be interpreted as a metallaazaridine-2-one with a trigonal-bipyramidal coordination sphere around iron, in which ethylene and N2 occupy the apical positions of the bipyramid. There is only one complex of this kind reported in the literature which was characterized by X-ray crystallography. It is a molybdenum compound with two phenyl-isocyanato ligands coordinated side-on along with a macrocyclic ligand coordinated by four sulfur atoms.[21]

The energetically most unfavorable intermediate we identified in the calculations of the approach of ethylene towards **S** from the base of the complex is $\mathbf{I_{13}}$, which is produced in an endothermic reaction from **S** and ethylene (72.5 kcal mol^{-1}, Figures 3 and 7). The system avoids the steric constraint induced by the approach of ethylene by means of an interaction of two terminal CO ligands to produce a C_2O_2 ligand. The structure may also be described as a trigonal-bipyramidal arrangement of the ligands around iron with N1 and the remaining CO ligand (C1) occupying the apical positions. To the best of our knowledge, such a transition-metal complex has not yet been reported in the literature. The most similar compounds are two tantalum complexes with dihydroxyacetylene ligands described by Lippard et al.[22]

Another possible approach of a molecule of ethylene towards **S** would be, of course, towards one of the triangular planes that forms the apex of the square-pyramid. If ethylene is moved towards **S** in the direction of the plane formed by the nitrogen atoms of the diazabutadiene ligand and the CO moiety adopting the apical position of the square-pyramid, the formation of $\mathbf{I_7}$ is observed. This reaction proceeds via the transition state $\mathbf{TS_2}$, which is also depicted in Figure 5. The activation energy is determined to be 47.3 kcal mol^{-1} (Figure 3). In $\mathbf{TS_2}$, the coordination sphere around iron still shows a square-pyramidal arrangement. Corresponding to the formation of an acyl ligand, the CO moiety is no longer linear but is bent to an angle of 139.4°. The Fe–C1 bond length of this CO group is also significantly longer than the corresponding bonds of the other terminal CO ligands because of the decreased back-bonding (185.8 pm versus 179.0 and 179.5 pm). In addition, the interaction of ethylene with the

0947-6539/03/0905-1176 $ 20.00+.50/0 *Chem. Eur. J.* **2003**, *9*, No. 5

diazabutadiene unit leads to significant changes in the bond lengths of the ligand. Thus, the C4–C5 bond (143.0 pm) as well as the N1–C4 bond (134.9 pm) of the imine unit interacting with ethylene are elongated compared to **S**, whereas the N2–C5 bond (130.6 pm) is shortened.

The molecular structure of $\mathbf{I_7}$ (Figures 3 and 6,) again shows an iron complex of square-pyramidal geometry with the acyl ligand occupying the apical position. The Fe-C1-O1 bond angle is 126.6°, the bond lengths of the tridentate ligands show the expected values. Thus, the former imine double bond between N1 and C4 now clearly represents a single bond (145.1 pm), whereas the second imine double bond is shortened compared to the situation in the starting complex **S** as a result of the loss of delocalization (N2–C5, 127.9 pm). The Fe–N bond lengths have different values, whereby the coordination of the amido nitrogen atom N1 is 13.1 pm shorter than the corresponding bond length of the imine nitrogen atom N2.

Although the formation of $\mathbf{I_7}$ directly from the approach of ethylene towards **S** via $\mathbf{TS_2}$ would give an intermediate in which the two new C–C bonds observed in the experimental catalytic reactions are already present, the attack of ethylene from the base of **S** leading to $\mathbf{I_4}$ via $\mathbf{TS_1}$ is the energetically more favorable path, since the activation energy is 4.7 kcal mol^{-1} lower (Figure 3). Therefore, in order to form $\mathbf{I_7}$ from $\mathbf{I_4}$, one of the equatorial CO ligands in $\mathbf{I_4}$ has to insert into the Fe–C bond which was formed by the previous interaction of ethylene with **S**. Because one of the CO (C2–O2) ligands in $\mathbf{I_4}$ is situated *trans* to an imine nitrogen atom (N2),whereas the other one (C1 – O1) is in a *trans* position with respect to an amide nitrogen atom (N1), there should be a difference in reactivity. Therefore, the reaction coordinates for both the potential insertion reactions have been calculated (Scheme 3). In $\mathbf{I_4}$, the two CO ligands show different distances to C6 (C1–C6 277.0 pm, C2–C6 265.5 pm). If C1 inserts into the Fe–C6 bond of $\mathbf{I_4}$, the transition state $\mathbf{TS_3}$ is observed, and the activation barrier for this process affords 19.9 kcal mol^{-1} (Table 3). On the other hand, the insertion of C2 into the Fe–C6 bond of $\mathbf{I_4}$ leads to the transition state $\mathbf{TS_4}$, the activation energy now reduces to 14.0 kcal mol^{-1}. Thus, the reaction via $\mathbf{TS_4}$ is energetically more favorable by 5.9 kcal mol^{-1}. The structures of $\mathbf{TS_3}$ and $\mathbf{TS_4}$ are shown in Figures 5 and 6, respectively. It is obvious that the bonding in $\mathbf{TS_4}$ between the inserting CO ligand and the former ethylene moiety as well as the interaction between C6 and the iron centre are stronger than in $\mathbf{TS_3}$. The fact that the insertion of the CO ligand *trans* to the imine group is preferred to the insertion of the CO group *trans* to the amide does not only reflect the steric situation in $\mathbf{I_4}$. This behavior also shows the importance of the *trans*-effect of the imine ligand, which is the better π acceptor compared to the amide ligand. Following the reaction coordinates, the transition states $\mathbf{TS_3}$ and $\mathbf{TS_4}$ both lead to the formation of $\mathbf{I_7}$. This process of CO insertion corresponds very well with results that have been achieved in earlier work which showed that the migratory insertion of CO involves a three-centre transition state, and the exothermicity of these processes was estimated to be ≈10 kcal mol^{-1} for first-row transition metals.[23]

The addition of another CO ligand to $\mathbf{I_7}$ leads to the coordinatively saturated complex $\mathbf{I_8}$, the reaction being endothermic by 6.0 kcal mol^{-1} as a consequence of entropic effects (Figures 3 and 4, Table 3). $\mathbf{I_8}$ shows an octahedral coordination mode of iron. The bond lengths and angles inside the tridentate ligand are very similar to the values observed in $\mathbf{I_7}$. It is obvious that the coordination of the ligands to iron is weaker than in $\mathbf{I_7}$. Both N–C bond lengths as well as the bond lengths of the acyl ligand to iron are longer than in $\mathbf{I_7}$. In addition, the CO ligand *trans* to the acyl function (C4–O4) shows the longest C–Fe bond of the three terminal CO ligands (Fe–C4 190.3 pm).

The formation of the experimentally observed heterocyclic products **P** may proceed via two different mechanisms. The first possibility is a reductive elimination which generates **P** by establishing a new bond between N1 and C1 and a highly reactive [Fe(CO)$_3$] fragment. This [Fe(CO)$_3$] fragment then might react with a diazabutadiene molecule to produce **S** again thus closing the catalytic cycle. In order to achieve the thermodynamics of this conceivable reaction pathway, **P** as well as the [Fe(CO)$_3$] fragment were calculated (Table 2, Figure 7). The conformation of the imine moiety of **P** with respect to the lactam ring is determined by a hydrogen bond between N2 and the amide hydrogen (N2–H1 254.1 pm). The

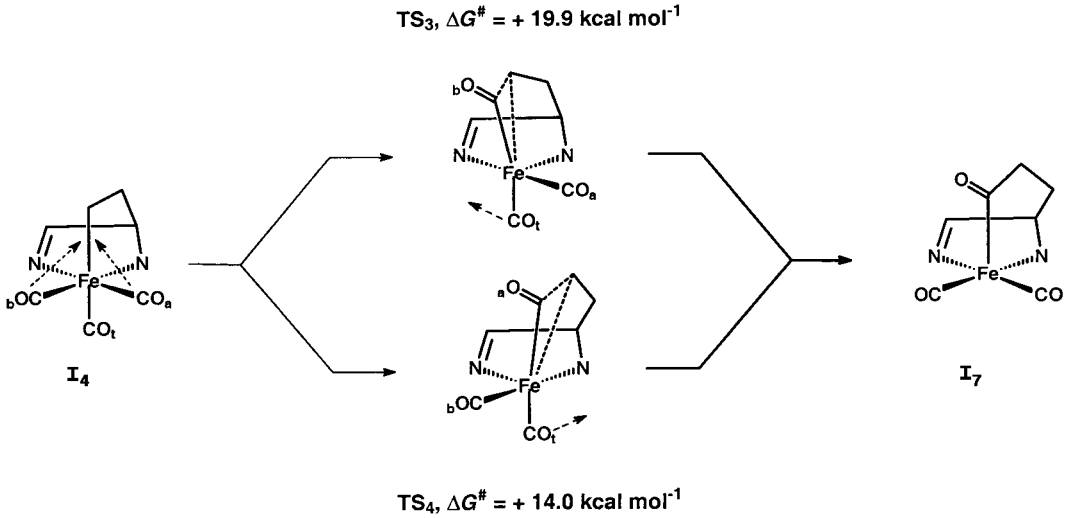

Scheme 3. Two different reaction courses of the insertion of an equatorial CO ligand in $\mathbf{I_4}$ into the Fe–C bond to give to $\mathbf{I_7}$

  0947-6539/03/0905-1177 $ 20.00+.50/0

relative energies show that a dissociation of $\mathbf{I_8}$ into **P** and $[Fe(CO)_3]$ would be an endothermic process with an overall free reaction energy of 3.9 kcal mol^{-1} (Figure 3).

The second possibility which might explain the formation of **P** is the closure of the N1–C1 bond in the coordination sphere of iron leading to $\mathbf{I_9}$ via $\mathbf{TS_5}$ (Figures 3 and 6). If, in $\mathbf{I_8}$, N1 is moved towards C1, the transition state $\mathbf{TS_5}$ is produced; this represents an activation barrier of 8.62 kcal mol^{-1} (Table 3). In $\mathbf{TS_5}$, the calculated N1–C1 distance is still 200.3 pm, whereas the bond between the the acyl moiety and the iron centre (C1–Fe 207.3 pm) is only shortened slightly by 2.8 pm compared to that in $\mathbf{I_8}$. In contrast to $\mathbf{I_8}$, in which the coordination mode around the iron centre is nearly octahedral, in $\mathbf{TS_5}$ N1 is moved out of the Fe-N2-C2-C3 plane by 99.1 pm. On the other hand, all CO ligands show an increased bond strength towards iron in $\mathbf{TS_5}$ compared to $\mathbf{I_8}$, which leads to shorter C–Fe bond lengths.

The ring closure between C1 and N1 converges in the formation of $\mathbf{I_9}$ (Figures 3 and 6). The overall reaction of $\mathbf{I_8}$ to form $\mathbf{I_9}$ is exothermic by 20.0 kcal mol^{-1}. In $\mathbf{I_9}$, the heterocyclic lactam still acts as a bidentate ligand through the lone pairs of the amide nitrogen N1 and the imine nitrogen N2. The coordination sphere around iron shows a trigonal-bipyramidal geometry with the imine nitrogen N2 and one of the CO ligands (C2–O2) occupying the apical positions. The most significant changes in the bond lengths are shown by the two N–Fe interactions. Compared to the situation in $\mathbf{I_8}$, the bond between the imine nitrogen atom N2 and the iron centre is 4.3 pm shorter in $\mathbf{I_9}$. In addition, the bonding between the iron centre and the nitrogen atom in the heterocycle (N1) is 31.0 pm longer than it was in $\mathbf{I_8}$ before the ring closure.

A dissociation of $\mathbf{I_9}$ into **P** and a $[Fe(CO)_3]$ fragment would be endothermic by 23.8 kcal mol^{-1} (Figure 3). On the other hand, the quite weak interaction between the amide nitrogen atom in $\mathbf{I_9}$ and iron clearly indicates the position in which an attack of a diazabutadiene might take place. This reaction coordinate results in the formation of $\mathbf{I_{10}}$, which is slightly exothermic (0.5 kcal mol^{-1}, Figures 3 and 6). In $\mathbf{I_{10}}$, the diazadiene as well as the lactam both act as mono-dentate ligands. The coordination sphere around iron is trigonal-bipyramidal with the exocyclic imine function of the product **P** adopting one of the apical positions. The bond lengths of the lactam ligand are nearly identical with those of noncoordinated **P** with the exception of the N2–C6 double bond, which is 1.3 pm longer in $\mathbf{I_{10}}$ than in **P** because of the coordination of the nitrogen lone pair to the iron center. The calculated torsional angle N2-C6-C5-N1 is 32.6° in $\mathbf{I_{10}}$, whereas this exocyclic imine moiety is nearly coplanar with the lactam ring in $\mathbf{I_9}$, $\mathbf{I_{11}}$ and **P**.

The coordination of the second imine function of the diazabutadiene ligand in $\mathbf{I_{10}}$ to the iron center leads to the liberation of the product **P** and to the formation of the starting compound **S**. As an intermediate of this process we identified $\mathbf{I_{11}}$, in which **P** still interacts with **S** through a hydrogen bond between the imine nitrogen atom of **P** and one of the hydrogen atoms attached to the imine nitrogen atoms of the diazabutadiene ligand (Figures 3 and 7). As expected, the formation of $\mathbf{I_{11}}$ from $\mathbf{I_{10}}$ is highly exothermic by 34.9 kcal mol^{-1} showing the high tendency of the system to form **S** by using the diazabutadiene as a chelating ligand again (Table 3). The bond lengths in $\mathbf{I_{11}}$ are nearly identical to the values calculated for the isolated molecules **P** and **S** (Figures 4 and 7). In another exothermic process (5.8 kcal mol^{-1}, Figure 3, Table 3) the hydrogen bond in $\mathbf{I_{11}}$ is broken to produce **P** and **S** as isolated species. According to our calculations, the overall reaction of $\mathbf{I_9}$ with a diazabutadiene results in the formation of **P** and **S** and is highly exothermic by 41.2 kcal mol^{-1}, thus representing the driving power of the whole catalytic reaction.

All calculations reported here were carried out assuming singlet ground states for the iron carbonyl compounds. This is justified in our opinion since it has been shown before that closed-shell singlets are the most stable structures for iron carbonyls.[10c] In addition, it is well-accepted that B3LYP is the most accurate method for determining thermochemical as well as vibrational data if iron carbonyl fragments are involved.[10b,c] Nevertheless, we calculated the key intermediate $\mathbf{I_7}$ with a triplet ground state for iron ($\mathbf{I_{7T}}$, Table 2). In analogy with reported results, we also found this intermediate to be less stable by 18.0 kcal mol^{-1} than the corresponding singlet state ($\mathbf{I_7}$) at the B3LYP/6-311++G(d,p) level. As expected, the triplet ground state also shows a large degree of iron–ligand repulsion as indicated by bond lengthening and a significantly distorted coordination geometry for iron. It is also worth mentioning that, even if the triplet ground states were more stable than the electronic structures we assumed for the intermediates and transition states of this catalysis, we are just comparing different reaction channels by their relative energy differences. Therefore, a consideration of the triplet ground states for all compounds calculated herein will certainly not lead to any substantial changes in the mechanism.

Conclusion

We were able to show by means of density functional theory at the B3LYP/6-311++G(d,p) level that the catalytic [2+2+1] cycloaddition reaction between a diazabutadiene, carbon monoxide and ethylene proceeds via a series of mononuclear iron carbonyl complexes. The starting point of the catalytic cycle is the [(diazabutadiene)$Fe(CO)_3$] complex **S** of square-pyramidal geometry. A closely related compound was characterized by X-ray diffraction and the results have been used to prove that the level of theory we chose for the calculations is suitable for compounds of this type since the calculated and experimentally observed bond lengths, angles and even torsional angles are essentially identical.

Interestingly, the catalytic reaction does not start with CO dissociation followed by an addition of ethylene and subsequent intramolecular reactions since this reaction pathway leads into a "dead-end" situation producing the highly strained intermediate $\mathbf{I_5}$, which readily decomposes to yield $\mathbf{I_2}$ again.

The more reasonable reaction channel is the approach of ethylene towards the base of the square-pyramidal starting complex. This reaction produces the intermediate $\mathbf{I_4}$ in which a new C–C bond between ethylene and one of the imine carbon atoms of the diazabutadiene is established along with a

0947-6539/03/0905-1178 $ 20.00+.50/0 *Chem. Eur. J.* **2003**, *9*, No. 5

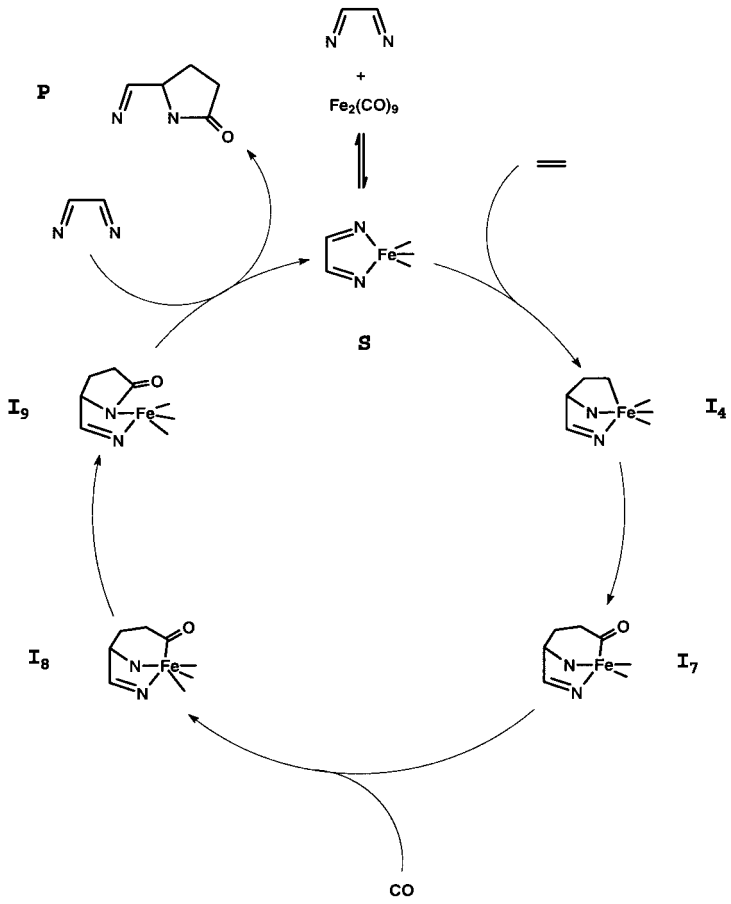

Scheme 4. Catalytic cycle of the [2+2+1] cycloaddition reaction of a diazabutadiene, carbon monoxide and ethylene generating lactams (substituents at nitrogen atoms have been omitted for the sake of clarity).

C–Fe interaction with the remaining ethylene carbon atom. An intramolecular CO insertion into the new C–Fe bond produces the electronically unsaturated 16-valence-electron compound $\mathbf{I_7}$ which readily adds one molecule of carbon monoxide to yield the octahedral complex $\mathbf{I_8}$.

Our calculations indicate that the experimentally observed lactams **P** with an additional exocyclic imine moiety are formed by a metal-assisted pathway. The intermediate $\mathbf{I_9}$ shows the lactam still acting as a bidentate ligand with the N–Fe bond from the amide nitrogen atom being quite weak. This bond is attacked by another diazabutadiene molecule to produce the free lactam **P** and the starting compound **S** again, and thus closing the catalytic cycle. The complete catalytic cycle that we postulate on the basis of our calculations is shown in Scheme 4.

In addition, the high-level DFT calculations we performed showed the existence of additional reaction channels that might be selectively accessible by employing appropriate reaction conditions and precatalysts or suitable substitution patterns of the substrates. Experimental work is in progress to prove these assumptions.

Experimental Section

General: All procedures were carried out under an argon atmosphere in freshly distilled anhydrous solvents. The preparation of glyoxaldiylidene-bis(-4-methoxyaniline) was carried out according to reference [24]. Infrared spectra were recorded on a Perkin Elmer FT-IR System 2000 in 0.2-mm KBr cuvettes. NMR spectra were recorded on a Bruker AC200 spectrometer (^{1}H: 200 MHz, ^{13}C: 50.32 MHz, $CDCl_3$ as internal standard) and on a Bruker DRX400 spectrometer (^{1}H: 400 MHz, ^{13}C: 100.62 MHz with $CDCl_3$ as internal standard). Mass spectra were recorded on a Finnigan MAT SSQ 710 instrument. High-resolution mass spectra were recorded on a Finnigan MAT 95 XL using ESI techniques and methanol as the solvent. Elemental analyses were carried out at the Institute of Organic and Macromolecular Chemistry of the Friedrich-Schiller-University, Jena (Germany).

X-ray crystallography: The structure determination of **3** was carried out on an Enraf Nonius Kappa CCD diffractometer, crystal detector distance 25 mm, 180 frames, graphite-monochromated $Mo_{K\alpha}$ radiation. The crystal was mounted in a stream of cold nitrogen. Data were corrected for Lorentz and polarization effects, but not for absorption. The structure was solved by direct methods and refined by full-matrix least-squares techniques against F^2 with the programs SHELXS 86 and SHELXL 93.[25] The molecular illustrations were drawn with the program XP.[26] The crystal and intensity data are given as a footnote.[27]

CCDC-177821 contains the supplementary crystallographic data for this paper. These data can be obtained free of charge via www.ccdc.cam.ac.uk/conts/retrieving.html (or from the Cambridge Crystallographic Data Centre, 12 Union Road, Cambridge CB2 1EZ, UK; fax: (+44) 1223-336033; or deposit@ccdc.cam.uk).

General procedure for catalytic cycloaddition reactions: In a typical experiment, *N*,*N*′-bis-(*p*-tolyl)-tetrahydropyrrolo-[2,1c][1,4]oxazine-3,4-diylidenediamine (1 mmol, 333 mg) was dissolved in toluene (3 mL). The solution was transferred together with $[Fe_2(CO)_9]$ (0.04 mmol, 15 mg) into a 75-mL stainless steel autoclave. The autoclave was evacuated and then pressurized with 13 atm CO and 8 atm ethylene. The reaction mixture was heated to 140 °C for 16 h. After the autoclave had cooled to room temperature, the pressure was released and the solution was transferred into a Schlenk tube. Then toluene was evaporated leaving a brown oily residue. This residue was used to determine the yield of the spirolactam **2** by NMR spectroscopy to be 55 % along with 45 % of the starting compound **1**. Analytical data for the compound derived from *N*,*N*′-bis-(*p*-tolyl)tetrahydropyrrolo[2,1c][1,4]oxazine-3,4-diylidenediamine have already been published by some of us.[5] Experiments with CO as the only gaseous reactant were performed as described, but without ethylene. The reactions with only ethylene were performed as for the typical experiment, but without CO. If the experiment was performed reacting cylohexylcyclohexylidene amine (1 mmol, 179 mg) with CO and ethylene, the ^{13}C NMR spectrum showed that not all of the starting compound had been consumed during the reaction and, in addition, that there are at least six different product compounds present on account of the observation of six resonances beneath the corresponding peak of the starting material in the region typical for keto or imine carbon atoms.

Preparation of 3: $[Fe_2(CO)_9]$ (0.5 g, 1.37 mmol) was suspended in a Schlenk tube in *n*-heptane (40 mL) together with glyoxaldiylidene-bis(-4-methoxyaniline) (0.44 g, 1.65 mmol). The mixture was heated to 50 °C for 45 min. The color of the solution changed from pale yellow to deep red. After all volatile material had been evaporated in vacuo, the oily residue was chromatographed on silica gel. With light petroleum (b.p. 40–60 °C) and

CH_2Cl_2 in a 2:1 ratio, **3** is obtained as a deep red solution. **3** may be recrystallized at −20 °C from light petroleum and CH_2Cl_2 in a 4:1 ratio (yield: 120 mg, 22 %). M.p. 130 °C (decomp); elemental analysis (%) calcd: C 55.91, H 3.95, N 6.86; found: C 55.28, H 4.06, N 6.71; MS (EI) (*m*/*z*) (fragment, %): 408 ($[M]^+$, 6), 380 ($[M-CO]^+$, 10), 352 ($[M-2CO]^+$, 37), 324 ($[M-3CO]^+$, 100), 267 ($[C_{16}H_{15}N_2O_2]^+$, 4), 162 ($[C_{11}H_{14}O]^+$, 49), 148 ($[C_{10}H_{12}O]^+$, 8), 134 ($[C_9H_{10}O]^+$, 25), 120 ($[C_8H_8O]^+$, 15), 106 ($[C_7H_6O]^+$, 8), 92 ($[C_6H_4O]^+$, 9), 77 ($[C_6H_5]^+$, 13), 56 ($[Fe]^+$, 36); IR (CH_2Cl_2, 298 K): $\tilde{\nu}$ = 2034 (s), 1959 (br, s) cm^{-1}; ^1H NMR ($CDCl_3$, 298 K): δ = 3.85 (s, 6H, OCH_3), 6.86–7.03 (m, 4H; $C_{ar}H$), 7.34–7.50 (m, 4H; $C_{ar}H$), 7.58 ppm (s, 2H; N=CH); ^{13}C NMR ($CDCl_3$, 298 K): δ = 55.0 (OCH_3), 113.3 ($C_{ar}H$), 123.6 ($C_{ar}H$), 144.0 (C_{ar}), 150.2 (N=CH), 157.2 (C_{ar}), 209.7 (CO), 211.9 ppm (CO).

Calculations: Full geometry optimizations (i.e. without symmetry constraints) were carried out with the GAUSSIAN 98 program package[28] and a hybrid Hartree–Fock DFT approach (B3LYP/6-311++G(d,p)) throughout.[29] The density functional employed contains a term which accounts for the effects of dynamic electron correlation (Coulomb hole).[30] The use of a basis set with triple ζ quality[31] and which contains diffuse functions is necessary because of the consideration of weakly bound (i.e. van der Waals) complexes, hydrogen-bridged species and a variety of interacting electron lone pairs. The B3LYP functional has previously been found to be of suitable theoretical level for the study of the interactions of transition metals with ligands, especially with CO.[32] To assess the reliability of the B3LYP/6-311++G(d,p) method, we 1) compared the X-ray structural data of complex **3** with results calculated at the B3LYP/6-311++G(d,p) level and 2) calculated the structures of $\mathbf{I_9}$, **P**, **S**, $\mathbf{TS_1}$, $\mathbf{TS_2}$, $\mathbf{TS_4}$, 1,4-diazabutadiene, and ethene with the standard augmented correlation-consistent triple ζ (aug-cc-pVTZ) basis set as defined by Dunning et al.[33] For the iron center we used a relativistic ECP of the SD group (SDD)[34] in conjunction with the [2f,1g] set.[35] The equilibrium geometries calculated with the B3LYP/aug-cc-pVTZ and the B3LYP/6-311++G(d,p) procedures compare remarkably well (see Table 2).[36] Relative energies, for example, as calculated for the ligand-exchange reaction ($\mathbf{I_9}$ + diazabutadiene → **S** + **P**), only differ to within 1 kcal mol^{-1} (ΔE = −43.42 kcal mol^{-1} (B3LYP/6-311++G(d,p)), −43.84 kcal mol^{-1} (B3LYP/aug-cc-pVTZ)). Thus, the B3LYP/6-311++G(d,p) approach appears to be an acceptable compromise as the aug-cc-pVTZ method would have significantly exceeded our contingent of CPU time.

In most cases B3LYP/LANL2DZ[37] optimizations were used to generate suitable starting geometries. Interestingly, in many cases, the LANL2DZ structures and (to a lesser extent), relative energies compare quite well with the 6-311++G(d,p) results. Stationary points were rigorously characterized as minima or transition states according to the number of imaginary modes by application of a second-order derivative calculation (vibrational analysis).[38] Visualization of the reactive mode in the transition structures was used to support the assignments of the pertaining minimum structures. Zero-point energy (ZPE) corrections have been made.

Thermochemistry calculations were performed with the standard routine in Gaussian 98, Version A11 (for details, see the Gaussian 98 User's Reference, Gaussian Inc., Carnegie Office Park, Building 6, Pittsburg, PA, USA) or the *freqchk* routine in conjunction with the final checkpoint file resulting from successful frequency calculations.[14, 15]

Acknowledgements

The authors gratefully acknowledge financial support by the Deutsche Forschungsgemeinschaft (Collaborative Research Center "Metal-Mediated Reactions Modeled after Nature", SFB 436). We also thank Dr. Sten Nilsson Lill and Dipl.-Chem. Stephan Schenk for fruitful discussions.

[1] a) M. Lautens, W. Klute, W. Tam, *Chem. Rev.* **1996**, *96*, 49; b) I. Ojima, M. Tzamariaoudaki, Z. Li, R. J. Donovan; *Chem. Rev.* **1996**, *96*, 635; c) O. Geis, H. G. Schmalz, *Angew. Chem.* **1998**, *110*, 955; *Angew. Chem. Int. Ed.* **1998**, *37*, 911; d) N. Jeong, *Trans. Met. Org. Synth.* **1998**, *1*, 560; e) Y. K. Chung, *Coord. Chem. Rev.* **1999**, *188*, 297; e) K. Brummond, J. L. Kent, *Tetrahedron* **2000**, *56*, 3263; f) A. J. Fletcher, S. D. R. Christie, *J. Chem. Soc. Perkin Trans. 1* **2000**, 1657.

[2] a) I. U. Khand, G. R. Knox, P. L. Pauson, W. E. Watts, M. I. Foreman, *J. Chem. Soc. Perkin Trans.* **1973**, 977; b) N. E. Schore, *Chem. Rev.* **1988**, *88*, 1081; c) P. L. Pauson, *Tetrahedron* **1985**, *41*, 5855; c) I. U. Khand, P. L. Pauson, *J. Chem. Soc. Chem. Commun.* **1974**, 379; d) I. U. Khand, P. L. Pauson, *Heterocycles* **1978**, *11*, 59; e) N. E. Schore in *Comprehensive Organic Synthesis* (Ed.: B. M. Trost), Oxford **1991**, *Vol. 5*, 1037.

[3] a) D. C. Billington, *Tetrahedron Lett.* **1983**, *24*, 2905; b) P. Magnus, L. M. Principe, M. J. Slater, *J. Org. Chem.* **1987**, *52*, 1483; c) D. C. Billington, W. J. Kerr, P. L. Pauson, C. F. Farnochi, *J. Organomet. Chem.* **1988**, *356*, 213; d) S. E. MacWhorther, V. Sampath, M. M. Olmstead, N. E. Schore, *J. Org. Chem.* **1988**, *53*, 203; e) V. Rautenstrauch, P. Megrard, J. Conesa, W. Kuster, *Angew. Chem.* **1990**, *102*, 1441; *Angew. Chem. Int. Ed. Engl.* **1990**, *29*, 1413; f) N. Jeong, S. H. Hwang, Y. Lee, *J. Am. Chem. Soc.* **1994**, *116*, 3159; g) B. Y. Lee, Y. K. Chung, N. Jeong, Y. Lee, S. H. Hwang, *J. Am. Chem. Soc.* **1994**, *116*, 8793; h) N. Y. Lee, Y. K. Chung, *Tetrahedron Lett.* **1996**, *37*, 3145; i) B. L. Pagenkopf, T. Livinghouse, *J. Am. Chem. Soc.* **1996**, *118*, 2285; k) N. Jeong, S. H. Hwang, Y. W. Lee, J. S. Lim, *J. Am. Chem. Soc.* **1997**, *119*, 10549; l) J. W. Kim, Y. K. Chung, *Synthesis* **1998**, 142; m) T. Sugihara, M. Yamaguchi, *J. Am. Chem. Soc.* **1998**, *120*, 10782; n) F. A. Hicks, N. M. Kablaoui, S. L. Buchwald, *J. Am. Chem. Soc.* **1996**, *118*, 9450; o) F. A. Hicks, S. L. Buchwald, *J. Am. Chem. Soc.* **1996**, *118*, 11688; p) Y. Koga, T. Kobayashi, K. Narasaka, *Chem. Lett.* **1998**, 249; q) N. Jeong, S. Lee, B. K. Sung, *Organometallics* **1998**, *17*, 3642.

[4] a) N. Chatani, T. Morimoto, Y. Fukumoto, S. Murai, *J. Am. Chem. Soc.* **1998**, *120*, 5335; b) N. Chatani, T. Morimoto, A. Kamitani, Y. Fukumoto, S. Murai, *J. Organomet. Chem.* **1999**, *579*, 177; c) W. E. Crowe, A. T. Vu, *J. Am. Chem. Soc.* **1996**, *118*, 1557; d) N. M. Kablaoui, F. A. Hicks, S. L. Buchwald, *J. Am. Chem. Soc.* **1996**, *118*, 5818; e) N. M. Kablaoui, F. A. Hicks, S. L. Buchwald, *J. Am. Chem. Soc.* **1997**, *119*, 4424; f) S. K. Mandal, S. R. Amin, W. E. Crowe, *J. Am. Chem. Soc.* **2001**, *123*, 6457; g) N.Chatani, M. Tobisu, T. Asaumi, Y. Fukumoto, S. Murai, *J. Am. Chem. Soc.* **1999**, *121*, 7160.

[5] A. Göbel, W. Imhof, *J. Chem. Soc. Chem. Commun.* **2001**, 593.

[6] G. M. Gordon, M. Kiszka, I. R. Dunkin, W. J. Kerr, J. S. Scott, J. Gebicki, *J. Organomet. Chem.* **1988**, *554*, 147.

[7] a) F. Robert, A. Milet, Y. Gimbert, D. Konya, A. E. Greene, *J. Am. Chem. Soc.* **2001**, *123*, 5396; b) M. Yamanaka, E. Nakamura, *J. Am. Chem. Soc.* **2001**, *123*, 1703; c) T. J. M. de Bruin, A. Milet, F. Robert, Y. Gimbert, A. E. Greene, *J. Am. Chem. Soc.* **2001**, *123*, 7184.

[8] a) E. R. Gamzu, T. M. Hoover, S. I. Gracon, *Drug. Dev. Res.* **1989**, *18*, 177; b) P. L. Dupont, J. Lamotte-Brasseur, O. Dideberg, H. Campsteyn, M. Vermeire, *Acta Crystallogr. Sect. B* **1977**, *33*, 1801; c) J. Leclercq, M.-W. De Pauw-Gillet, R. Bassleer, L. Angenot, *J. Ethnopharmacol.* **1986**, *15*, 305; d) *The Alkaloids: Chemistry and Biology*, *Vol. 5*, (Ed.: G. A. Cordell), **1998**, Academic, San Diego; e) P. B. Alper, C. Meyers, A. Lerchner, D. R. Siegel, E. M. Carreira, *Angew. Chem.* **1999**, *111*, 3379; *Angew. Chem.Int. Ed. Engl.* **1999**, *38*, 3186.

[9] See: S. Niu, M. B. Hall, *Chem. Rev.* **2000**, *100*, 353, and references therein.

[10] a) H. Jacobsen, T. Ziegler, *J. Am. Chem. Soc.* **1996**, *118*, 4631; b) J. H. Jang, J. G. Lee, H. Lee, Y. Xie, H. F. Schaefer, III, *J. Phys. Chem. A* **1998**, *102*, 5298; c) Y. Xie, H. F. Schaefer, III, R. B. King, *J. Am. Chem. Soc.* **2000**, *122*, 8746.

[11] a) V. Pank, J. Klaus, K. von Deuten, M. Feigel, H. Bruder, H. tom Dieck, *Transition Met. Chem.* **1981**, *6*, 185; b) H.-W. Frühauf, G. Wolmershauser, *Chem. Ber.* **1982**, *115*, 1070; c) B. Chaudret, H. Koster, R. Poilblanc, *J. Chem. Soc. Dalton Trans.* **1983**, 941; d) H. tom Dieck, W. Kollvitz, I. Kleinwächter, W. Rohde, L. Stamp, *Transition Met. Chem.* **1986**, *11*, 361; e) A. Romero, A. Vegas, A. Santos, M. Martinez-Ripoll, *J. Organomet. Chem.* **1987**, *319*, 103; f) H. tom Dieck, H. Bruder, E. Kuhl, D. Junghans, K. Hellfeldt, *New. J. Chem.* **1989**, *13*, 259; g) M. J. Blandamer, J. Burgess, J. Fawcett, P. Guardado, C. D. Hubbard, S. Nuttall, L. J. S. Prouse, S. Radulovic, D. R. Russell, *Inorg. Chem.* **1992**, *31*, 1383; h) P. P. M. de Lange, M. J. A. Kraakman, M. van Wijnkoop, H.-W. Frühauf, K. Vrieze, W. J. J. Smeets, A. L. Spek, *Inorg. Chim. Acta* **1992**, *196*, 151; i) M. J. A. Kraakman, B. de Klerk-Engels, P. P. M. de Lange, K. Vrieze, W. J. J. Smeets, A. L. Spek, *Organometallics* **1992**, *11*, 3774; j) H. A. Nieuwenhuis, M. C. E. van de Ven, D. J. Stufkens, A. Oskam, K. Goubitz, *Organometallics* **1995**, *14*, 780; k) M. Menon, A.

  0947-6539/03/0905-1180 $ 20.00+.50/0 *Chem. Eur. J.* **2003**, *9*, No. 5

Pramanik, A. Chakravorty, *Inorg. Chem.* **1995**, *34*, 3310; l) M. van Wijnkoop, P. P. M. de Lange, H.-W. Frühauf, K. Vrieze, W. J. J. Smeets, A. L. Spek, *Organometallics* **1995**, *14*, 4781; m) M. P. Aarnts, M. P. Wilms, K. Peelen, J. Fraanje, K. Goubitz, F. Hartl, D. J. Stufkens, E. J. Baerends, A. Vlcek, Jr., *Inorg. Chem.* **1996**, *35*, 5468; n) M. P. Aarnts, A. Oskam, D. J. Stufkens, J. Fraanje, K. Goubitz, N. Veldman, A. L. Spek, *J. Organomet. Chem.* **1997**, *531*, 191; o) P. Le Floch, F. Knoch, F. Kremer, F. Mathey, J. Scholz, W. Scholz, K.-H. Thiele, U. Zenneck, *Eur. J. Inorg. Chem.* **1998**, 119; p) C. J. Kleverlaan, D. J. Stufkens, J. Fraanje, K. Goubitz, *Eur. J. Inorg. Chem.* **1998**, 1243; q) W. Imhof, A. Göbel, R. Beckert, T. Billert, H. Görls, *J. Organomet. Chem.* **1999**, *590*, 104; r) J. Breuer, H.-W. Frühauf, W. J. J. Smeets, A. L. Spek, *Inorg. Chim. Acta* **1999**, *291*, 438;

[12] M. W. Kokkes, D. J. Stufkens, A. Oskam, *J. Chem. Soc. Dalton Trans.* **1983**, 439.

[13] H.-W. Frühauf, J. Breuer, *J. Organomet. Chem.* **1984**, *277*, C13.

[14] For a brief introduction see: a) J. W. Ochterski, Gaussian Inc. **1999**, 1; b) J. W. Ochterski, Gaussian Inc. **2000**, 1; c) P. Y. Ayala, H. B. Schlegel, *J. Chem. Phys.* **1997**, *108*, 2314.

[15] While the correction for entropy turns out to be of significant importance for the catalytic cycle discussed in this paper, the dependence of relative energies from corrected values calculated for elevated temperatures and pressures appear to be of minor influence, see, for example, the values for $T = 438$ K and $p = 10$ atm in the Supporting Information.

[16] a) D. Braga, F. Grepioni, K. Biradha, V. R. Pedireddi, G. R. Desiraju, *J. Am. Chem. Soc.* **1995**, *117*, 3156; b) D. Braga, F. Grepioni, G. R. Desiraju, *Chem. Rev.* **1998**, *98*, 1375; c) W. Imhof, A. Göbel, D. Braga, P. De Leonardis, E. Tedesco, *Organometallics*, **1999**, *18*, 736; d) D. Berger, M. Erdmann, J. Notni, W. Imhof, *CrystEngComm.* **2000**, 4; e) G. R. Desiraju, T. Steiner, *The Weak Hydrogen Bond*, Oxford University Press **1999**.

[17] a) H. Wawersik, F. Basolo, *J. Am. Chem. Soc.* **1967**, *89*, 4626; b) J. A. S. Howell, P. M. Burkinshaw, *Chem. Rev.* **1983**, *83*, 557; c) F. Basolo, *Inorg. Chim. Acta* **1985**, *100*, 3; d) T. R. Herrington, T. L. J. Brown, *J. Am. Chem. Soc.* **1985**, *107*, 5700; e) W. C. Trogler, *Int. J. Chem. Kinet.* **1987**, *19*, 1025; f) M. C. Baird, *Chem. Rev.* **1988**, *88*, 1217; g) F. Basolo, *Pure Appl. Chem.* **1988**, *60*, 1193; h) F. Basolo, *Polyhedron*, **1990**, *9*, 1503; i) Z. Lin, M. B. Hall, *Inorg. Chem.* **1992**, *31*, 2791; j) J. Li, G. Schreckenbach, T. Ziegler, *J. Am. Chem. Soc.* **1995**, *117*, 486; k) S. F. Lincoln, A. E. Merbach, *Adv. Inorg. Chem.* **1995**, *42*, 1.

[18] a) E. Lindner, E. Schauss, W. Hiller, R. Fawzi, *Angew. Chem.* **1984**, *96*, 727; *Angew. Chem. Int. Ed. Engl.* **1984**, *23*, 711; b) E. Lindner, E. Schauss, W. Hiller, R. Fawzi, *Chem. Ber.* **1985**, *118*, 3915; c) M. Brookhart, W. A. Chandler, A. C. Pfisterer, C. C. Santini, P. S. White, *Organometallics* **1992**, *11*, 1263; d) F. Meier-Brocks, R. Albrecht, E. Weiss, *J. Organomet. Chem.* **1992**, *439*, 65.

[19] B. de Klerk-Engels, J. G. P. Delis, J.-M. Ernsting, C. J. Elsevier, H.-W. Frühauf, D. J. Stufkens, K. Vrieze, K. Goubitz, J. Fraanje, *Inorg. Chim. Acta* **1995**, *240*, 273.

[20] a) L. H. Staal, G. van Koten, K. Vrieze, B. van Santen, C. H. Stam, *Inorg. Chem.* **1981**, *20*, 3598; b) F. Muller, G. van Koten, K. Vrieze, B. Krijnen, C. H. Stam, *J. Chem. Soc. Chem. Commun.* **1986**, 150; c) F. Muller, G. van Koten, K. Vrieze, *Organometallics* **1989**, *8*, 33; d) F. Muller, G. van Koten, K. Vrieze, D. Heijdenrijk, B. B. Krijnen, C. H. Stam, *Organometallics* **1989**, *8*, 41; e) M. van Wijnkoop, R. Siebenlist, J. M. Ernsting, P. P. M. Lange, H.-W. Frühauf, E. Horn, A. L. Spek, *J. Organomet. Chem.* **1994**, *482*, 99; f) P. P. M. de Lange, R. P. de Boer, M. van Wijnkoop, J. Ernsting, H.-W. Frühauf, K. Vrieze, W. J. J. Smeets, A. L. Spek, K. Goubitz, *Organometallics* **1993**, *12*, 440.

[21] T. Yoshida, T. Adachi, K. Kawazu, A. Yamamoto, N. Sasaki, *Angew. Chem.* **1991**, *103*, 1025; *Angew. Chem. Int. Ed. Engl.* **1991**, *30*, 982.

[22] a) R. N. Vrtis, C. P. Rao, S. G. Bott, S. J. Lippard, *J. Am. Chem. Soc.* **1988**, *110*, 7564; b) R. N. Vrtis, S. G. Bott, R. L. Rardin, S. J. Lippard, *Organometallics* **1991**, *10*, 1364.

[23] a) K. Koga, K. Morokuma, *Chem. Rev.* **1991**, *91*, 823; b) H. Berke, R. Hoffmann, *J. Am. Chem. Soc.* **1978**, *100*, 7224; c) P. Hofmann, P. Stauffert, K. Tatsumi, A. Nakamura, R. Hoffmann, *Organometallics* **1985**, *4*, 404; d) P. Hofmann, P. Stauffert, K. Tatsumi, A. Nakamura, R. Hoffmann, *J. Am. Chem. Soc.* **1985**, *107*, 4440; e) M. D. Curtis, K.-B. Shiu, W. M. Butler, *J. Am. Chem. Soc.* **1986**, *108*, 1550; f) T. Ziegler, L. Versluis, V. Tschinke, *J. Am. Chem. Soc.* **1986**, *108*, 612; g) F. U. Axe, D. S. Marynick, *Organometallics* **1987**, *6*, 572; h) F. U. Axe, D. S. Marynick, *J. Am. Chem. Soc.* **1988**, *110*, 3728; i) S. Sakaki, K. Kitaura, K. Morokuma, K. Ohkabo, *J. Am. Chem. Soc.* **1983**, *105*, 2280; j) N. Koga, K. Morokuma, *J. Am. Chem. Soc.* **1985**, *107*, 7230; k) N. Koga, K. Morokuma, *J. Am. Chem. Soc.* **1986**, *108*, 6136; l) A. K. Rappé, *J. Am. Chem. Soc.* **1987**, *109*, 5605; m) M. R. A. Blomberg, C. A. M. Karlsson, P. E. M. Siegbahn, *J. Phys. Chem.* **1993**, *97*, 9341; n) Z. X. Zao, S. Q. Niu, M. B. Hall, *J. Phys. Chem. A* **2000**, *104*, 7324.

[24] L. N. Ferguson, T. C. Goodwin, *J. Am. Chem. Soc.* **1949**, *71*, 633.

[25] a) G. Sheldrick, SHELXS-86, Universität Göttingen **1986**; b) G. Sheldrick, SHELXL-93, Universität Göttingen **1993**.

[26] Siemens Analytical X-ray Inst. Inc., XP - Interactive Molecular Graphics, Vers. 4.2, **1990**.

[27] Crystal and intensity data for **2**: $T = 183$ K, deep red crystal, crystal size $0.34 \times 0.32 \times 0.30$ mm, orthorhombic, $a = 6.5019(3)$, $b = 25.333(1)$, $c = 11.0440(3)$ Å, $V = 1819.1(1)$ Å^3, $Z = 4$, $F(000) = 840$, $\rho_{calcd} = 1.490$ g cm^{-3}, space group *Pnma*, $\mu = 0.862$ mm^{-1}, $\theta = 3.04 - 23.24°$, ϕ- and ω-scan, 4276 reflections measured, 1326 independent reflections, 1234 observed reflections $F_o^2 > 2\sigma(F_o^2)$, 160 parameters, GOOF = 1.177, $R_1 = 0.0362$, $wR_2 = 0.1012$, final diff. map electron density 0.372 e Å^{-3}.

[28] Gaussian 98, Revision A11, M. J. Frisch, G. W. Trucks, H. B. Schlegel, G. E. Scuseria, M. A. Robb, J. R. Cheeseman, V. G. Zakrzewski, J. A. Montgomery, Jr., R. E. Stratmann, J. C. Burant, S. Dapprich, J. M. Millam, A. D. Daniels, K. N. Kudin, M. C. Strain, O. Farkas, J. Tomasi, V. Barone, M. Cossi, R. Cammi, B. Mennucci, C. Pomelli, C. Adamo, S. Clifford, J. Ochterski, G. A. Petersson, P. Y. Ayala, Q. Cui, K. Morokuma, D. K. Malick, A. D. Rabuck, K. Raghavachari, J. B. Foresman, J. Cioslowski, J. V. Ortiz, B. B. Stefanov, G. Liu, A. Liashenko, P. Piskorz, I. Komaromi, R. Gomperts, R. L. Martin, D. J. Fox, T. Keith, M. A. Al-Laham, C. Y. Peng, A. Nanayakkara, C. Gonzalez, M. Challacombe, P. M. W. Gill, B. Johnson, W. Chen, M. W. Wong, J. L. Andres, C. Gonzalez, M. Head-Gordon, E. S. Replogle, and J. A. Pople, Gaussian, Inc., Pittsburgh PA, **1998**.

[29] A. D. Becke, *J. Chem. Phys.* **1993**, *98*, 5648.

[30] C. Lee, W. Yang, R. G. Parr, *Phys. Rev. B* **1988**, *37*, 785.

[31] R. S. Grev, H. F. Schaefer, III, *J. Chem. Phys.* **1989**, *91*, 7305.

[32] a) A. D. Becke, *J. Chem. Phys.* **1992**, *97*, 9173; b) P. E. M. Siegbahn, M. R. A. Bomberg, *Chem. Rev.* **2000**, *100*, 421.

[33] R. A. Kendall, R. J. Harrison, T. H. Dunning, *J. Chem. Phys.* **1992**, *96*, 6796.

[34] M. Dolg, U. Wedig, H. Stoll, H. Preuss, *J. Chem. Phys.* **1987**, *86*, 866.

[35] J. M. L. Martin, A. Sundermann, *J. Chem. Phys.* **2001**, *114*, 3408.

[36] For the compatibility of correlation-consistent basis sets with hybrid HF/DFT methods: see: K. S. Raymond, R. A. Wheeler, *J. Comput. Chem.* **1999**, *20*, 207.

[37] a) P. J. Hay, W. R. Wadt, *J. Chem. Phys.* **1985**, *82*, 270; b) P. J. Hay, W. R.Wadt, *J. Chem. Phys.* **1985**, *82*, 284; c) P. J. Hay, W. R. Wadt, *J. Chem. Phys.* **1985**, *82*, 299.

[38] P. Pulay in *Ab initio methods in quantum chemistry* (Ed.: K. P. Lawley), Wiley, New York, **1987**, p. 241.

Received: July 18, 2002
Revised: November 5, 2002 [F4257]